AD NUMBER

AD874223

NEW LIMITATION CHANGE

TO

Approved for public release, distribution unlimited

FROM

Distribution: Further dissemination only as directed by Army Materiel Command, ATTN: AMCPA-S, Washington, DC 20315, APR 1970, or higher DoD authority.

AUTHORITY

AMC ltr dtd 26 Dec 1973

AD _____

RDTE PROJECT 1S665702D625-05

USATECOM PROJECT 9-CO-005-000-002

METHODOLOGY INVESTIGATION:
OUTPUT CHARACTERISTICS
OF THE WHITE SANDS MISSILE RANGE
FAST BURST REACTOR

FINAL REPORT

BY

TED F. LUERA
DON L. WELCH

APRIL 1970

INFORMATION ONLY
Action By Higher Authority Pending

ARMY MISSILE TEST AND EVALUATION
WHITE SANDS MISSILE RANGE
NEW MEXICO

DISPOSITION INSTRUCTIONS

Destroy this report when it is no longer needed. Do not return it to the originator. The disposition instructions do not apply to the record copy.

DISCLAIMER

The use of trade names in this report does not constitute an official endorsement or approval of the use of such commercial hardware or software. This report may not be cited for purposes of advertisement.

Information and data contained in this document are based on input available at the time of preparation. Because the results may be subject to change, this document should not be construed to represent the official position of the US Army Materiel Command unless so stated.

DISTRIBUTION

Each transmittal of this document within US Army Materiel Command must have prior approval of CG, USATECOM, ATTN: AMSTE-TS, Aberdeen Proving Ground, Maryland 21005. Each transmittal of this document outside US Army Materiel Command must have prior approval of CG, US Army Materiel Command, ATTN: AMCPA-S, Washington, DC 20315.

RDTE PROJECT 1S665702D625-05

USATECOM PROJECT 9-CO-005-000-002

METHODOLOGY INVESTIGATION:

OUTPUT CHARACTERISTICS

OF THE WHITE SANDS MISSILE RANGE

FAST BURST REACTOR

TEST REPORT

BY

TED F. LUERA
DON L. WELCH

APRIL 1970

ARMY MISSILE TEST AND EVALUATION
WHITE SANDS MISSILE RANGE
NEW MEXICO

iii

ABSTRACT

The results of neutron and gamma radiation dosimetry measurements
are presented in this report. Sufficient data are provided so that
estimates of the neutron fluence, neutron spectrum, gamma dose, and
gamma dose rate can be obtained for both burst operations and power
runs.

A discussion of the dosimetry techniques presently in use at the
Nuclear Effects Directorate is presented, as are plans for improving
and expanding upon these techniques.

A summary of those factors which affect burst yield or maximum power
level is also provided.

FOREWORD

The Fast Burst Reactor Division of the Nuclear Effects Directorate
(NED), Army Missile Test and Evaluation, White Sands Missile Range,
was responsible for the planning and performance of these tests and for
the preparation of this report.

The assistance of all personnel who helped in the gathering of data and
in the preparation of the report is gratefully acknowledged. Special
recognition is extended to personnel of the NED Dosimetry Section for
their assistance and cooperation in obtaining dosimetry data and pro-
viding information on dosimetry procedures.

TABLE OF CONTENTS

Table of Contents (cont)

Table of Contents (cont)

ix

SECTION 1. SUMMARY

1.1 BACKGROUND

a. The Fast Burst Reactor Division is an operational element of the Nuclear Effects Directorate, Army Missile Test and Evaluation, White Sands Missile Range. The Fast Burst Reactor Facility (FBRF) is used for the performance of radiation effects tests, including the evaluation of electronic systems and components, radiobiological studies, and determination of effects on materials. The Nuclear Effects Directorate (NED) provides instrumentation and dosimetry support for the user of its facilities.

b. This report presents the results of recent dosimetry measurements made at the FBRF. Data contained herein are based on calibrations performed by the NED Dosimetry Section.

c. The radiation environment produced by the FBR is affected by the presence of experiments near the reactor. The data presented here are appropriate for the conditions under which they were taken. The estimates obtained from this report should be supplemented by the results of dosimetry measurements made under the desired experimental conditions. Further, the correlation of experimental effects with exposure depends on the knowledge of the neutron energy spectrum. The free-field integral energy spectrum is provided in this report. Energy deposition and hence damage effects are proportional to the flux weighted cross sections of the material being irradiated. Therefore, when objects massive enough to significantly alter the spectrum are exposed, spectral data should be obtained for proper interpretation of results (para 2.1.3.2).

1.2 DESCRIPTION OF MATERIEL

a. The FBR is an unmoderated and unreflected fast burst (or prompt pulse) reactor designed to be operated in the super-prompt-critical region. It can also be operated in a steady-state (power) mode. Operations are normally conducted in a cell that is 50 feet square and 20 feet high, but facilities are also available for outdoor operation. There are no features of the surrounding terrain that limit the utility of the outdoor site.

b. The reactor core consists of six cylindrical stacked and bolted fuel rings, three control elements, and a safety block. These core components are 93.2% enriched in uranium-235 and alloyed with ten weight percent molybdenum (U—10 wt. % Mo). The control elements move axially in the core on a 3.125-inch radius (Fig. 1). The cylindrical safety block moves along the axis of the core into the stacked fuel assembly. The core is shielded with a cadmium-covered mild steel decoupling shroud, or safety shield, which also acts as a cooling air plenum. The core is cooled by forced air convection.

c. Three thermocouples are used to monitor the reactor core temperature. These thermocouples are located in the core as follows:

(1) T_1 (chromel-alumel), axially in the safety block

(2) T_2 (chromel-alumel), axially through the four bottom fuel rings

(3) T_3 (iron-constantan), radially in the fourth ring from the bottom

d. The quantity ΔT_3 has been used as the reference temperature change to specify burst yield. The data in this report are referenced to ΔT_1 since T_1 can be more directly related to the peak fuel temperature (T_p). Conversion from one thermocouple reading to another can be readily made because the ratios of thermocouple readings have been constant. The ratios are:

$$\frac{\Delta T_1}{\Delta T_p} = 0.99$$

1-2

RETAINING PLATE (SS)

ASSEMBLY BOLT (3)

MASS ADJUSTMENT RING

CENTER INSERT (U-Mo)

STEPPED ANNULAR DISKS (6) (U-Mo)

CONTROL ROD (2) (U-Mo)

SUPPORT PLATE (SS)

VENT HOLE

AIR FLOW GROOVES

BURST ROD (U-Mo)

THERMOCOUPLE HOLE

SAFETY BLOCK (U-Mo)

SAFETY BLOCK MANDREL (SS)
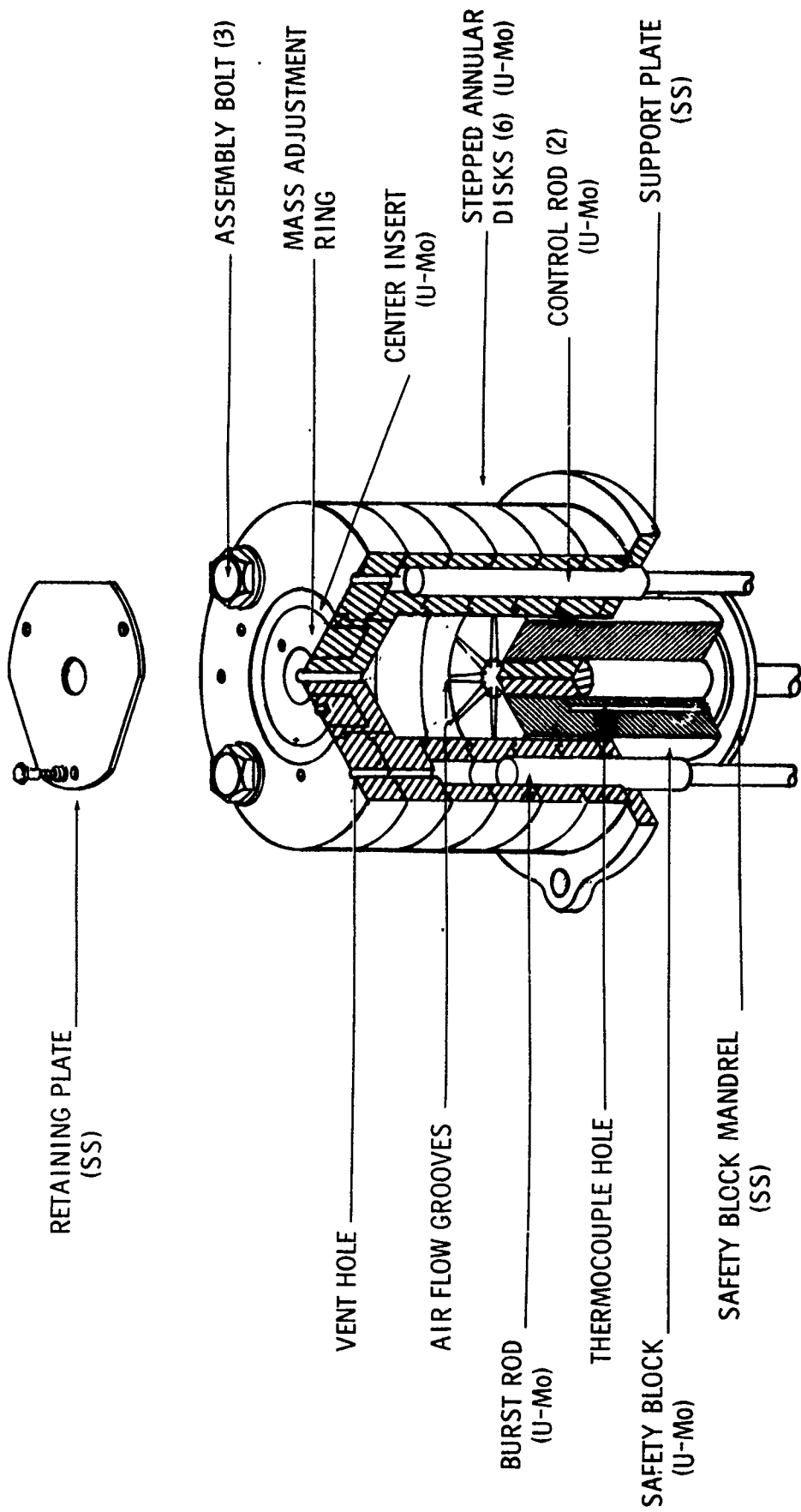
Figure 1. Isometric section of FBR core.

$$\frac{\Delta T_1}{\Delta T_2} = 1.33$$

$$\frac{\Delta T_1}{\Delta T_3} = 1.18$$

$$\frac{\Delta T_2}{\Delta T_3} = 0.88$$

Thes. thermocouple ratios are in good agreement with the fission density distribution in the core obtained by a two-dimensional (r, z) neutron transport code calculation (Ref 1*).

e. A modification of the FBR being planned for the first quarter of FY 71 will include the insertion of spacers between the fuel rings to reduce axial shock effects. The reduction of these shock effects will make it feasible to perform bursts of higher yield. In addition, the safety block mandrel will be modified so that the safety block will be supported from the bottom. Modification of the center insert will then provide an internal irradiation cavity that is 1.25 inches in diameter and approximately 7 inches long. This cavity will be reduced to about 1.0 inch in diameter by the necessary liners. It is anticipated that the fluence in this cavity will approach 10^{15} fast neutrons per square centimeter, as compared to less than 10^{14} at the closest external experimental approach. A new safety shield is being designed for installation on the FBR stand in conjunction with the core modification. This safety shield will employ 155 mg/cm^2 of boron-10 as decoupling material.

f. Most FBR burst operations are in the range between 210° and 300°C (ΔT_1). Pulsewidths are typically 40 to 50 microseconds full-width

---

*References are listed in Appendix II.

at half-maximum (FWHM). In the presence of moderating materials, pulses over 200 microseconds wide can be obtained (para 2. 3. 3. 1). Fission yields are typically on the order of 10^{17} fissions. The minimum time between bursts is limited to approximately 75 minutes by the efficiency of the forced-air cooling system. Of these 75 minutes, 20 are required for the decay of airborne contamination, and 30 are required for preparation of the reactor for burst. The remaining 25 minutes may be used by the experimenter for setting up, removing, or altering experiments in the cell. Few experimenters maintain this schedule; in general, the time between bursts is determined by the experimenter.

g. Trigger pulses usable for starting oscilloscope traces or for other experimenter requirements are available. These are adjustable from 900 seconds to a few microseconds prior to the burst peak.

h. Power operations up to 10 kilowatts are performed when high doses are required and dose-rate effects can be neglected.

i. After an operation, the reactor is shut down, lowered into a 38-foot-deep pit, and covered with a lead shielding door to provide for rapid recovery of exposed items.

j. For exposure, small items are placed on a 4- by 8-foot experiment table, which is adjustable in the vertical direction (Fig. 2). A hole has been cut through the center of the table so that the reactor can be brought up into position for operation after the test items are in place.

1.3 OBJECTIVES

a. The purpose of this report is to provide a reference for the determination of:

(1) The radiation environment produced by any given reactor operation

1-5
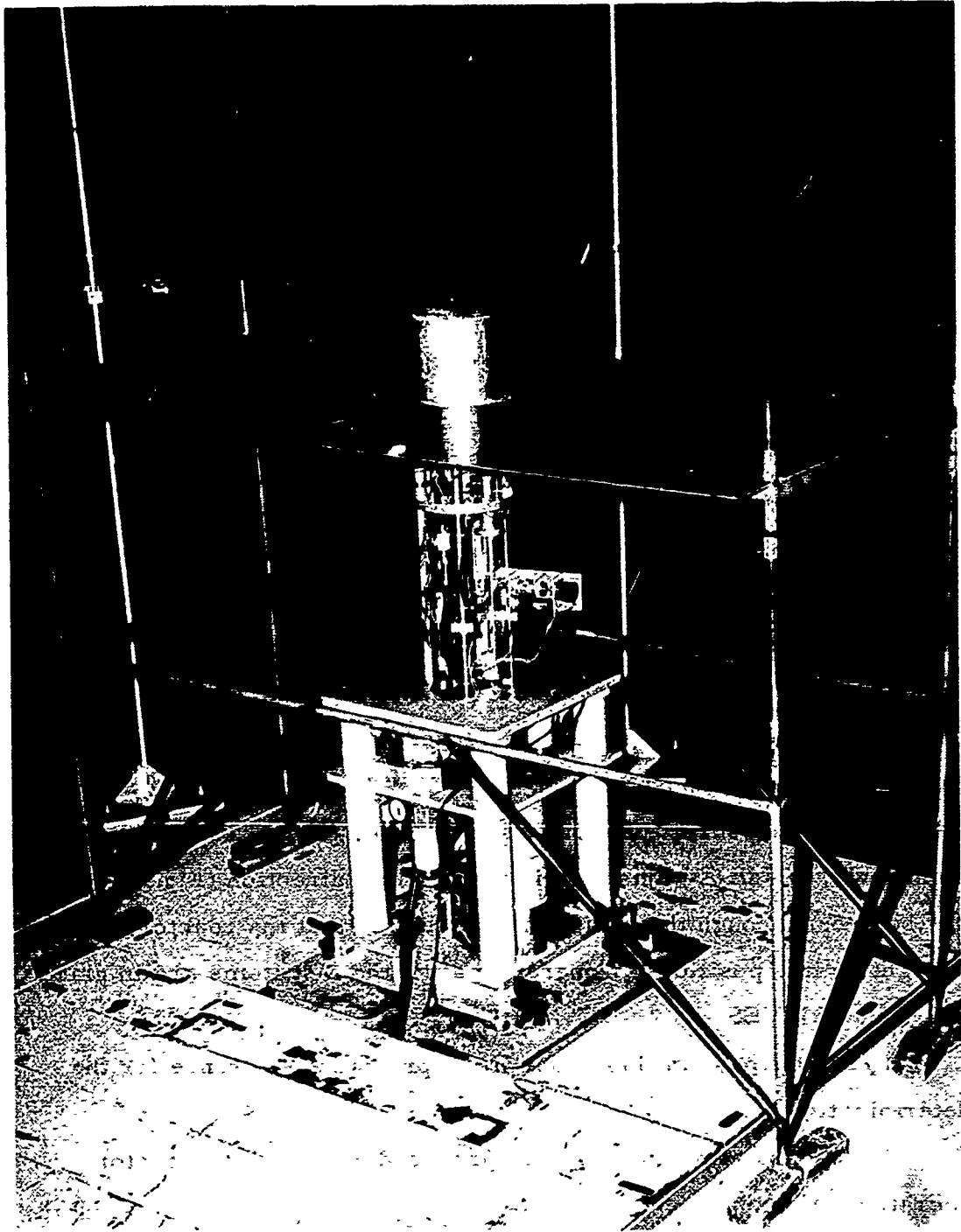
Fig. 2.   Fast Burst Reactor with Experiment Table

(2) The number, type, and fission yield of the reactor operations required to provide a given radiation environment

b. Additional information is provided to enable the user of the facility to design his experiment to fit the constraints imposed by the nuclear characteristics of the reactor.

1.4 SCOPE

a. This report presents the results of neutron and gamma dosimetry measurements made at the FBRF. It is intended for use by the facility contractor as an aid in planning and preparing for tests at the FBR, and by members of the reactor staff, primarily as a reference for dosimetry data.

b. Factors affecting the output characteristics of the reactor are summarized. Some data are provided on thermal characteristics and the effects of reflectors. Definitive and detailed investigations in these areas have not been completed.

1.5 SUMMARY OF RESULTS

a. The free-field neutron fluence and gamma exposure data obtained during these tests are in good agreement with previous measurements (Ref 2).

b. The results of the dosimetry measurements are summarized in tabular and graphic form in the appropriate sections of this report.

1.6 CONCLUSIONS

The following specific conclusions are derived from the dosimetry data obtained during these tests:

a. The recalibration of the sulfur dosimetry system (para 2.1.2) resulted in an increase of approximately 12% in the measured fluence for a given burst.

b. The recalculation of the power level for a given compensated ion chamber current (para 2.1.3.3) resulted in an increase of 16% in the neutron flux at a given power level.

1-7

c. Based on dosimetry measurements and heat capacity calculations, the efficiency of the in-core thermocouples is approximately 70%.

d. The gamma exposure rate for a given burst operation decreases approximately as $1/R^{1.7}$, where R is the distance between the detector and the reactor core centerline.

1.7 RECOMMENDATIONS

a. It is recommended that additional dosimetry measurements be made at the FBR. These should include high-resolution neutron spectrum measurements in both free-field and shielded configurations.

b. The neutron sensitivity of the LiF thermoluminescent dosimeters (TLDs) in use at NED should be evaluated.

c. A detailed study of the FBR thermal characteristics is required. Intrinsic thermocouples capable of following the burst temperature profile should be used to provide an accurate measure of the temperature rise in the core.

d. Radiochemical analysis of fission foils placed within the reactor core is required to provide additional insight into the number of fissions in the core for any given operation.

e. An investigation of the FBR modified core characteristics is required, as are dosimetry measurements within the internal irradiation cavity.

f. Measurements of the gamma-ray spectrum should be made for both free-field conditions and behind shields of commonly used materials.

SECTION 2. DETAILS OF TEST

2.1 NEUTRON DOSIMETRY

2.1.1 Objective

The objective of the neutron dosimetry measurements is to describe the neutron environment within the reactor cell for both burst and power operations.

2.1.2 Method

2.1.2.1 Sulfur Dosimetry

a. At present, sulfur activation is the primary method used to determine the neutron fluence at the FBR. If the neutron spectrum is known, the total fast-neutron fluence can be determined from the exposure of sulfur pellets. An effective threshold of 3 Mev is chosen for the ^{32}S (n, p) ^{32}P reaction (Ref 3).

b. Recalibration of the NED sulfur activation counting system was performed in 1969 with the Los Alamos Cockcroft-Walton accelerator as a source of monoenergetic neutrons (Ref 4). The neutron output of the Los Alamos Cockcroft-Walton is well known. A calibration, or counter, constant is determined for each sulfur counter by the relation

$$K = \frac{\sigma_0 \Phi_0}{\overline{\sigma} C_0}$$

where the subscripted variables are the cross section, fluence, and the initial beta count rate for the monoenergetic fluence, and $\overline{\sigma}$ is the average cross section for the spectrum in which the fluence is being measured. The fluence is calculated by the equation

$$\Phi_0 = K C_t e^{\lambda t}$$

where K is the counter constant, C_t is the count rate measured t days after the irradiation, and λ is $(0.693/14.2)\ d^{-1}$. As a result of this recalibration, the counter constants were increased by 12.5%. The errors

2-1

involved in fluence measurements with sulfur pellets are discussed in paragraph 2. 1. _. 8.

c. The pellets in use at NED are 3/4 inch in diameter, 1/4 inch thick, and are encased in a protective aluminum can. Pellets are beta counted 3 to 5 days after irradiation in one of two Nuclear Chicago counters or in a Beckman Widebeta-II. The wait period allows the ^{24}Na activity from the (n, a) reaction in the aluminum can and the ^{31}Si activity from the (n, a) reaction in ^{34}S to decay to a negligible level. Significant additional background activity is produced by the capture of thermal neutrons in ^{34}S. The half-lives of ^{24}Na, ^{31}Si, and ^{35}S are 15 hours, 2.6 hours, and 87 days, respectively. Because of the long half-life of ^{35}S, special techniques must be used to read pellets exposed in high thermal fluxes. A Digital Equipment Corporation PDP-8 computer is used to control the sequencing of the counters. The PDP-8 also calculates the fluence using the Sulflux I program, which makes corrections for counter geometry and efficiency and extrapolates the activity back to the time of exposure. Once the fluence is calculated, the data are stored on magnetic tape as a permanent record and are printed out by teletype to be forwarded to the experimenter. The PDP-8 can be programmed to count to a preset number of counts and used on a 24-hour-per-day basis. Neutron dosimetry is reported in time-integrated neutron flux or fluence (n/cm^2). A comparison of NED and EG&G sulfur dosimetry measurements was made by EG&G after the recalibration of the system. Approximately 50 measurements over a wide range of fluences were compared. Discrepancies in the measured values were systematic and were less than 2%.

2. 1. 2. 2 Thermal Neutron
          Measurements

a. Thermal neutron fluence measurements are made with gold activation foils that are exposed in pairs. One foil is inclosed in a

cadmium shield, and the other is unshielded.   Activation in the bare foil
is produced by both thermal and epithermal neutrons.   Ideally, activa-
tion in the covered foil is only by neutrons above the cadmium cutoff.
The difference in the foil activities is therefore proportional to the
thermal neutron fluence.   For a quantitative treatment of gold foil tech-
niques, see Reference 3.

   b.   The thermal neutron dosimetry system is currently available
for experimenter use.   The system will be recalibrated in 1970 as part
of an overall NED dosimetry recalibration program.

2.1.2.3 Spectrum Measurements

   a.   Recalibration of the fission foil counters is being carried out by
members of the Dosimetry Section.   In addition, a study is being con-
ducted to evaluate nickel foils as a substitute for sulfur pellets as the
primary means of fluence measurement.   Nickel foils are advantageous
in that they are smaller than sulfur pellets and, unlike sulfur, can be
read by gamma counting techniques.

   b.   The SPECTRA computer code is presently being adapted for use
at NED.   This code provides a smooth differential spectrum based on
foil activation measurements and a trial spectrum (Ref 5).

   c.   An Oak Ridge Technical Enterprises Corporation (ORTEC) ^{6}Li
neutron spectrometry system is presently being calibrated and will be
used to make free-field spectral measurements and measurements
behind shields of various materials in the reactor cell.   The ^{6}Li detector
uses the

$$\,_{0}^{1}n + \,_{3}^{6}Li \longrightarrow \,_{2}^{4}He + \,_{1}^{3}H + Q$$
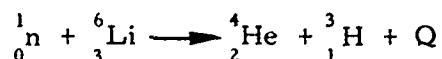
reaction, with the α particle and the triton counted in coincidence in
two silicon surface barrier detectors.   The pulses are shaped and
summed to provide an output proportional to the Q of the reaction plus

2-3

the incident neutron energy. Because the detector counts individual neutron events, it may be used only during steady-state operations of the reactor. An ORTEC ^{3}He spectrometry system has also been purchased for use at the NED facilities. The ^{3}He detector operation is based on the

$$\,^1_0 n + \,^3_2 He \longrightarrow \,^1_1 H + \,^3_1 H + Q$$
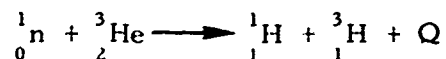
reaction. Its operation is similar to that of the ^{6}Li detector system. The ^{3}He system provides higher sensitivity and better energy resolution. This system will also be used during steady-state operations at the FBR.

d. A 38.5 cm^3 lithium drifted germanium solid-state detector is currently available for use in conjunction with a 4096-channel pulse-height analyzer. This system provides high-resolution (3.5 kev) energy spectrum analyses of activated samples.

2.1.3 Results

2.1.3.1 Spectral Measurements

The neutron fluence produced by the FBR has been measured by a series of foil activation measurements (Ref 2). The foils used were Pu, Np, U, S, Ni, Mg, and Al. The free-field spectral data are presented in Table I and are applicable to free-field conditions. Caution must be exercised in using the 8:1 plutonium-to-sulfur fluence ratio near the reactor cell walls (>190 inches from core centerline) or if the experiment being exposed can significantly change the neutron spectrum.

2.1.3.2 Conversion to Dose

a. For the Godiva spectrum, Reference 3 gives a value of

$$\frac{rad}{\Phi_{Pu}} = 2.5 \times 10^{-9} \frac{rads \ (tissue)}{n/cm^2}$$

for the conversion of plutonium fluence (Φ_{Pu}) to rads tissue. The sulfur

2-4

TABLE I

FBR NEUTRON SPECTRUM

AS DETERMINED BY THRESHOLD DETECTORS

Detector	^{239}Pu	^{237}Np	^{238}U	S or Ni	Mg	Al
Energy Threshold (Mev)	0.01	0.6	1.5	3.0	6.3	7.5
Percent Fluence Above Each Threshold	100	62	33	12.5	1.7	0.6
Percent Fluence in Each Energy Band	38	29	20.5	10.8	0.9	0.7

fluence (Φ_S) is 12.5% of the total fluence (Table I), and therefore the relation

$$\frac{rad}{\Phi_S} = 2.0 \times 10^{-8} \frac{rads\ (tissue)}{n/cm^2}$$

can be used to convert free-field sulfur fluence to dose in rads tissue. Since the Godiva spectrum is slightly more energetic than the FBR spectrum, these values overestimate the tissue dose by a few percent.

    b.   An estimate of the 1 Mev equivalent fluence in silicon was made by using the reactor free-field energy spectrum. The cross sections used were calculated from data in Reference 6. The following relation was used to calculate the weighting factors:

2-5

$$W_i = \frac{(\overline{E\sigma})_i}{E_1\sigma_1}$$

where $(\overline{E\sigma})_i$ is the average product of the energy times the elastic scattering cross section over the ith energy range.

c. The quantity $E_1\sigma_1$ is 1 Mev times the elastic scattering cross section for silicon at that energy. The results of the calculation are listed in Table II.

<center>

TABLE II

ONE MEV EQUIVALENT FLUENCE (SILICON)

</center>

Neutron Group (i)	Energy Range (Mev)	Fluence (%)	Relative Weight
1	0.01 - 0.6	36	0.418
2	0.6 - 1.5	30	0.969
3	1.5 - 3.0	22	2.02
4	3.0 - 6.3	10.6	2.27
5	6.3 - 7.5	1	2.05
6	7.5 - ∞	0.6	2.04

d. The relation

$$\Phi(\text{Equivalent}) = \frac{\sum\limits_{i=1}^{6} W_i \Phi_i}{\sum\limits_{i=1}^{6} \Phi_i}$$

<center>2-6</center>

yields

$$\Phi(1 \text{ Mev}) = 1.16 \, \Phi_{Pu} \, (>10 \text{ kev})$$

e. The conversion of fluence to first collision dose was obtained by the equation (Ref 3)

$$\frac{rad}{\Phi_{Pu}} = 1.602 \times 10^{-8} \, f \, N \sum_{i=1}^{6} (\overline{E\sigma})_i \, F_i$$

where Φ_{Pu} is the total fast fluence, f is the average fractional energy transfer per collision, N is the number of nuclei per gram in the sample, and F_i is the fraction of fluence in the ith energy band. The value

$$\frac{rad}{\Phi_{Pu}} = 7.76 \times 10^{-11} \frac{rads \, (silicon)}{n/cm^2}$$

was obtained for the FBR spectrum.

2.1.3.3 Normalization of Data

a. Neutron fluence as measured with sulfur pellets placed at a given position relative to the core varies linearly with fission yield. In order to simplify the use of data presented in this report, burst data are normalized to a 1-degree temperature change in T_1, and power run data are normalized to 1 kilowatt-minute. The errors resulting from normalization to ΔT_1 are small, as shown in Table III.

b. The power-level calibration was obtained by using the following equation:

$$\Phi_S = \frac{K_1 \, K_2}{4\pi R^2} Pt \times \frac{\Phi_S}{\Phi_{Pu}}$$

where K_1 is based on 190 Mev per fission and is equal to 3.28×10^{10} fissions per watt-second. The quantity K_2 is the number of lea'   ge neutrons

2-7

TABLE III

ERROR IN FLUENCE RESULTING FROM

NORMALIZATION TO ΔT_1 AS A FUNCTION OF T_1

T_1 (°C)	Error in Fluence (%)
25	+6.0
125	+4.5
187	+2.7
250	0.0

per fission and is approximately 1.48 neutrons per fission (Ref 4), P is the power level in watts, and t is the duration of the power run in seconds. The ratio Φ_S / Φ_{Pu} is found in Table I for the free-field spe⌐ .\m. Sulfur fluence measurements made at distances from 10 to 150 in were used to obtain an average value for the power level. The results of these measurements were used to plot power level versus current from the compensated ion chamber, which is used to monitor the neutron population in the reactor. This calibration curve is shown in Figure I-1 (Appendix I).

2.1.3.4 Radial Measurements

a. Free-field radial measurements were made in the midplane of the core with a thin metal ring and lacing cord string to the walls of the reactor cell. Sulfur pellets were suspended from the lacing cord. Measurements were taken during power runs and burst operations. The reported fluence is the time-integrated neutron flux greater than 3 Mev.

b. Fluence per kilowatt-minute as a function of radial distance from the core centerline is plotted in Figure I-2. The following equation can

be used to calculate the fluence from a power run:

$$\Phi_S \cong 4.38 \times 10^{12} \frac{Pt}{R^2}$$

where the units of P, t, and R are kilowatts, minutes, and inches, respectively. Radial fluence measurements for both burst operations and power runs deviate from $1/R^2$ behavior from the surface of the safety shield (4.5 inches) to 10 inches and at distances greater than 200 inches. Table IV lists the calculated fluence, the measured fluence, and percent difference as a function of distance from the core centerline for power runs.

TABLE IV

CALCULATED AND MEASURED
FLUENCE FOR POWER RUNS

Distance (in.)	Calculated Fluence per kw-min ($n/cm^2 > 3$ Mev)	Measured Fluence per kw-min ($n/cm^2 > 3$ Mev)	Error (%)
6.5	1.035×10^{11}	1.143×10^{11}	+10
10	4.37×10^{10}	4.51×10^{10}	+3
20	1.093×10^{10}	1.091×10^{10}	-0.3
50	1.75×10^{9}	1.68×10^{9}	-4
100	4.37×10^{8}	4.26×10^{8}	-3
150	1.949×10^{8}	1.98×10^{8}	+1
200	1.093×10^{8}	1.12×10^{8}	+2
250	7.00×10^{7}	7.86×10^{7}	+10

c. Neutron fluence per ΔT_1 is plotted as a function of radial distance from the core centerline in the core midplane in Figure I-3. The following equation can be used to calculate the approximate fluence from a burst:

$$\Phi_S = 8.25 \times 10^{11} \frac{\Delta T_1}{R^2}$$

where R is the distance to the core centerline in inches. Table V is a comparison of measured and calculated values.

TABLE V

CALCULATED AND MEASURED

FLUENCE FOR BURSTS

Distance (in.)	Calculated Fluence per ΔT_1 ($n/cm^2 > 3$ Mev)	Measured Fluence per ΔT_1 ($n/cm^2 > 3$ Mev)	Error (%)
6.5	1.95×10^{10}	2.14×10^{10}	+10
10	8.25×10^{9}	8.43×10^{9}	+2
20	2.06×10^{9}	2.03×10^{9}	-1
50	3.30×10^{8}	3.15×10^{8}	-5
100	8.25×10^{7}	8.33×10^{7}	-1
150	3.67×10^{7}	3.71×10^{7}	+1
200	2.06×10^{7}	2.16×10^{7}	+5
250	1.32×10^{7}	1.51×10^{7}	+13

2-10

2. 1. 3. 5 Vertical Distribution

Fluence measurements were made along vertical lines at 6 inches,
12 inches, and 1 meter from the core centerline.   Figures I-4 through
I-6 show the fluence distribution as a function of vertical distance from
the horizontal midplane of the core.   The experimenter table was in
position with the table surface 6 inches below the core midplane.   The
vertical distribution at 1 meter without the experimenter table is shown
in Figure I-7.   For these measurements, tape was stretched vertically
between two horizontal members on a large ring stand, and sulfur pellets
were held in place by the tape.   This technique insured that a minimum
number of scattered neutrons were counted.

2. 1. 3. 6 Angular Dependence

In Figure I-8, fluence as a function of angle is plotted for several dis-
tances.   The angles are referred to north and increase in a clockwise
direction as viewed from the top.   These measurements were made in
the horizontal midplane of the core.   Statistical errors were on the order
of 0. 2%, and the maximum deviation from the arithmetic mean was 7%.
The effects of positioning errors are superimposed on the flux distribu-
tion.   Fluence depressions correspond to locations of the inconel bolts.
These are located at 90, 210, and 330 degrees.   The maximum deviation
from symmetry is of the same order as the estimated positioning error
(para 2. 1. 3. 8).   At a distance of about 10 inches from the core axis,
these small depressions disappear, and the measured fluence attains
radial symmetry.

2. 1. 3. 7 Changes in Fluence
           Characteristics

Neutron fluence and gamma dose measurements were made behind
shields of thicknesses up to 9 inches in order to demonstrate the
variety of radiation environments obtainable from reactor operations.

2-11

The shields were planar slabs approximately 18 inches high by 24 inches long. The center of the shield and the dosimeters were in the midplane of the core. The front of the shield was always at 8 inches from the core centerline, and the dosimetry was at 17 inches for all measurements. Tables VI and VII show the results of these measurements.

2.1.3.8 Error in Sulfur Dosimetry Measurements

a. Uncertainties in the measured values of the neutron fluence at the FBR arise primarily from uncertainties in detector calibration, pellet size and weight, pellet counting, and positioning of the pellet.

b. The uncertainties in detector calibration result from errors in cross-section values, counting statistics, and errors in the source flux used for the calibration process. One method of detector calibration involves exposing a threshold detector with a known activation cross section to a monoenergetic source flux and determining the count rate at some time after irradiation. A calibration constant may then be evaluated as

$$K = \frac{\sigma_0 \Phi_0}{\overline{\sigma} C_0}$$

where σ_0 and C_0 are the cross section and initial count rate as determined by the source fluence Φ_0. The quantity $\overline{\sigma}$ is the average cross section for the flux spectrum where the detector will be exposed. The relative error in K arising from variation of the dependent variables is given by

$$\frac{\delta K}{K} = \pm \left[\left(\frac{\delta \sigma_0}{\sigma_0} \right)^2 + \left(\frac{\delta \overline{\sigma}}{\overline{\sigma}} \right)^2 + \left(\frac{\delta \Phi_0}{\Phi_0} \right)^2 + \left(\frac{\delta C_0}{C_0} \right)^2 \right]^{\frac{1}{2}}$$

and is estimated to be on the order of 12% for the case of sulfur pellet calibration.

2-12

TABLE VI

CHANGES IN FBR FLUENCE CHARACTERISTICS

Shield			Attenuation*	Neutron Ratio / Gamma	3 Mev / Thermal Ratio
Cadmium (mil)	Lead (mil)	Polyethylene (in.)	$\Phi > 3$ Mev	$\Phi > 3$ Mev $/ R_\gamma$	$\Phi > 3$ Mev $/ \Phi$ (thermal)
60	0	9	27	---	0.39
60	0	7.9	16	1.27×10^7	0.44
40	0	6.2	8	2.17×10^7	0.48
20	0	4.5	4.5	4.59×10^7	--
20	0	1.7	1.7	---	0.52
20	0	0.56	1.2	---	8.9
20	250**	0.56	1.3	5.23×10^8	4.3
0	0	0	1	4.75×10^8	--

*Not corrected for thermal neutron contribution to sulfur pellet reading
**In front

TABLE VII

CHANGE IN NEUTRON SPECTRUM

Shield		Percent of Fluence in Each Energy Band (Mev)			
Cadmium (mil)	Polyethylene (in.)	Thermal	0.01-1.5	1.5-3.0	3.0
60	9	24	55	10.5	10.5
0	0	<1	67	20.5	12.5

c. The relative error in the dimensions of a sulfur pellet is given by

$$\left[\left(\frac{2\delta r}{r} \right)^2 + \left(\frac{\delta w}{w} \right)^2 \right]^{\frac{1}{2}}$$

d. For a sulfur pellet 0.750 inch in diameter and 0.250 inch thick, the dimensional error to within 1/32 inch is less than 2%.

e. The dependence of K on the weight of a sulfur pellet is avoided by making the pellet "infinitely thick" to beta particles; that is, a beta particle of energy 1.7 Mev emitted at the back surface of the pellet would not be able to penetrate to the front surface (Ref 7).

f. The following expression is used to determine the fluence Φ_0 to which a pellet is exposed:

$$\Phi_0 = C_t \, e^{\lambda t} \times K$$

Here, C_t is the count rate obtained at an elapsed time t after exposure, and K is the calibration constant as previously defined. The error in the calculated value of the fluence is given by

$$\Phi_0 \pm \delta\Phi_0 = C_t \, e^{\lambda t} \, K \left[1 \pm \sqrt{ \left(\frac{\delta C_t}{C_t} \right)^2 + \left(\frac{\delta \, e^{\lambda t}}{e^{\lambda t}} \right)^2 + \left(\frac{\delta K}{K} \right)^2 } \right]$$

Assuming no error in counting time,

$$\frac{\delta C_t}{C_t} = \frac{\delta N}{N} = \frac{1}{\sqrt{N}}$$

where N is the total number of counts.

g. The exponential term reduces to $\delta(\lambda t)$, and for $\lambda t \ll 1$, that is, for counting times which are short compared to the half-life, the error in the exponential factor is negligible compared to errors in K and N.

2-14

h. The relative error in calculated fluence then reduces to

$$\frac{\delta\Phi_0}{\Phi_0} = \pm\left[\frac{1}{N} + \left(\frac{\delta K}{K}\right)^2\right]^{\frac{1}{2}}$$

i. For the instance where N is large (as is usually the case), the error in calculated fluence is primarily dependent upon the error in K .

j. For the case where the fluence follows a $1/r^2$ dependence, we may write

$$\Phi = \frac{c}{r^2}$$

k. An error in positioning of a pellet will produce an error in the measured value of the fluence, as seen in Figure 3.
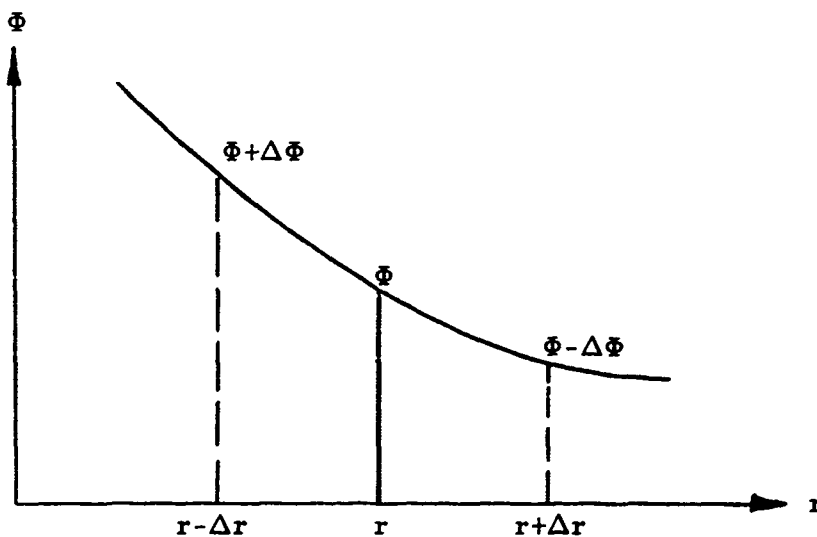

Fig. 3. Neutron Fluence as a Function of Distance

The error in the measured value of Φ at a point r due to an error Δr is

$$\Phi + \Delta\Phi = \frac{c}{(r - \Delta r)^2}$$

$$= \frac{c}{r^2}\left(1 - \frac{\Delta r}{r}\right)^{-2}$$

The maximum value of Φ due to an error Δr is then

$$\Phi_{max} = \Phi + \Delta\Phi \approx \frac{c}{r^2}\left(1 + \frac{2\Delta r}{r}\right)$$

In a like manner, the minimum value of Φ at a point r due to an error in r is

$$\Phi_{min} = \Phi - \Delta\Phi \approx \frac{c}{r^2}\left(1 - \frac{2\Delta r}{r}\right)$$

The ratio of Φ_{max} to Φ_{min} at r is

$$\frac{\Phi_{max}}{\Phi_{min}} = \left(\frac{1 + 2\Delta r/r}{1 - 2\Delta r/r}\right)$$

$$\approx \left(1 + \frac{2\Delta r}{r}\right)^2$$

1. The above ratio is shown in Figure 4 with a positioning error of 0.125 inch. The positioning errors become negligible at large distances, but at distances closer than about 10 inches, errors on the order of ±10% are not unlikely. Positioning errors are due in part to positioning of the experimenter table relative to the core and the positioning of the reactor by the reactor lift.

Figure 4. Error in neutron fluence due to an error in foil position, as a function of distance from the core centerline.
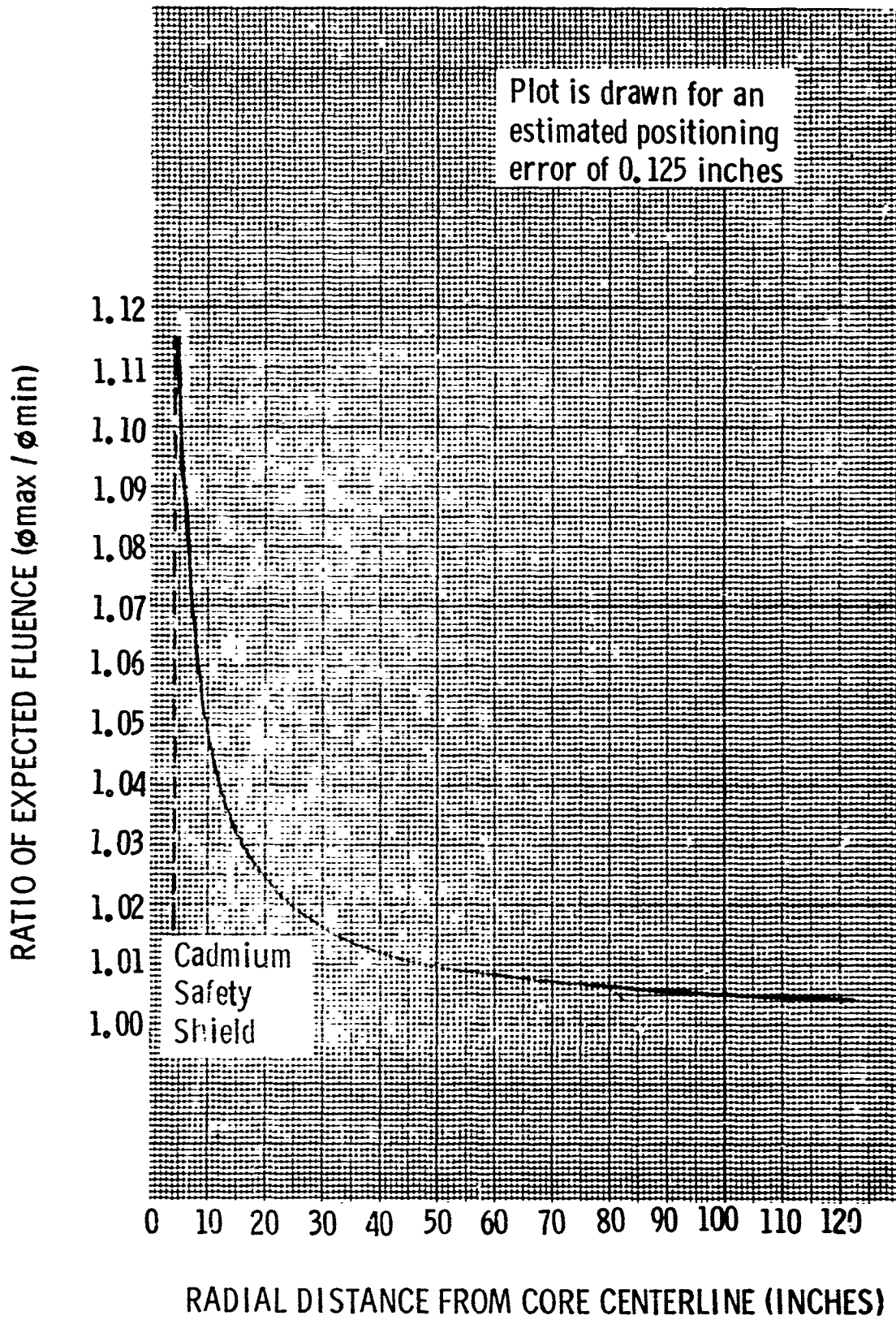
2.1.3.9 Calculation of Fission Yield

a. The number of fissions in the FBR core for a burst of $\Delta T_1 = 291°C$ was calculated by two independent techniques.

b. The number of fissions that take place in a burst can be calculated by the following equation:

$$\Phi_S = \frac{1.48}{4\pi R^2} \times F \times \frac{\Phi_S}{\Phi_{Pu}}$$

where Φ_S is the measured sulfur fluence (n/cm^2), Φ_S/Φ_{Pu} is the ratio of the sulfur fluence to the plutonium fluence under free-field conditions, R is the distance from the core centerline to the sulfur pellet, F is the number of fissions in the burst, and 1.48 is the number of leakage neutrons per fission (Ref 8).

c. The free-field burst data between 10 and 150 inches (Table V) was used to obtain an average value for $\Phi_S R^2$. The average value of Φ_S/Φ_{Pu} for these distances is 1/8.12 (Ref 2). The number of fissions calculated was

$$F (\Delta T_1 = 291°C) = 1.08 \times 10^{17}$$

d. The energy deposited in the fuel per fission and the heat capacity of the fuel were also used to determine the number of fissions in the core for this burst.

e. The energy required to change the temperature in the core from T_0 to T is given by (Ref 9)

$$\Delta Q = M \left[a\overline{\Delta T} + b\overline{\Delta T} (T + T_0) \right] \qquad \text{Eq (1)}$$

where M is the mass of U-10 wt. % Mo in the core $(96.5 \times 10^5 \text{ gm})$, a and b are constants, and $\overline{\Delta T}$ is the average temperature change of

2-18

the core. The number of fissions required to deposit this energy in the core is given by

$$F = \frac{\Delta Q}{K}$$

where the value of K is 178 Mev/fission (Ref 10). For ΔQ in fissions:

$$a = 4.72 \times 10^9$$

$$b = 2.60 \times 10^6$$

and, from Reference 1,

$$\overline{\Delta T} = \frac{\Delta T_1}{2.05}$$

When $\Delta T_1 = 291°C$ and $T_0 = 30°C$ are used,

$$F = 7.18 \times 10^{16} \text{ fissions}$$

f. If equation (1) is solved for $\overline{\Delta T}$, the following result is obtained:

$$\overline{\Delta T} = \frac{(a + 2bT_0) \pm \sqrt{(a + 2bT_0)^2 + 4bF/M}}{2b}$$

Substituting $F = 1.078 \times 10^{17}$ fissions into the above equation yields $\Delta T_1 = 427°C$.

g. The efficiency of the thermocouple for the burst can be defined as:

$$\epsilon = \frac{\Delta T_{1m}}{\Delta T_{1c}} = \frac{291}{427} \approx 70\%$$

where ΔT_{1m} is the measured temperature change, and ΔT_{1c} is the calculated value.

2-19

h. Since the thermocouple ratios are in good agreement with calculated values (para 1.2), the efficiencies of the other thermocouples (TC 2 and 3) may also be considered to be close to 70%. The apparent low efficiency of the thermocouples may be misleading since the errors in the calculated value are not small. The primary errors are dosimetry calibration (~12%), point source approximation (~5%), and assumption of uniform temperature rise in the core. However, the low efficiency can be attributed to the inability of the thermocouple to respond quickly enough to the change in temperature. This effect is enhanced by the presence of a brass shim between the thermocouple junction and the fuel. Until further measurements are made with, for example, intrinsic thermocouples, the following assumptions are made:

(1) The sulfur activation measurements provide the correct (larger) number of fissions.

(2) The heat capacity calculation based on this number of fissions yields the correct (higher) temperature.

i. The number of fissions in the core versus the measured and calculated values of ΔT_1 are plotted in Figure I-9.

2.2 GAMMA DOSIMETRY

2.2.1 Objective

The objective of the gamma dosimetry measurements is to describe the gamma-ray environment within the reactor cell for both burst and power operations.

2.2.2 Method

2.2.2.1 Lithium Fluoride and Lithium Borate

a. Lithium fluoride thermoluminescent dosimeters (TLD-700) are the primary means of gamma exposure equivalent measurements at the Nuclear Effects facilities. The lithium in TLD-700 powder is 99.993% pure ^{7}Li. Lithium fluoride powder is exposed in small cylindrical teflon containers.

b. Extensive cross-calibration with various facilities across the country was carried out early in 1969. Several hundred LiF and $Li_2B_4O_7$ dosimeters were sent to Kirtland Air Force Base, Sandia Corporation, Bell Telephone Laboratories, and Natick Laboratories for exposures to ^{60}Co of from 1 to 20 x 10^6 R. The results of this cross-calibration were very satisfactory and showed:

(1) Agreement within ±5% among all the facilities, including the WSMR reading

(2) Linearity of $Li_2B_4O_7$ extending to about 2 x 10^6 R (Ref 11)

c. Lithium fluoride exhibits a flat energy response over a wide range, with an excess response of approximately 25% at 15 kev. After exposure, the measured dose decreases by about 5% in 3 days and then becomes stable. The LiF powder is read on a modified Conrad reader. The heating time is 11 seconds at 300°C. The photomultiplier is on for 10.5 seconds, starting 0.25 second after the heating is begun and ending 0.25 second before the heating is terminated. Light output as measured

by the photomultiplier is plotted against ^{60}Co exposure as measured with an ionization chamber for calibration of the system.

    d.   The lithium borate TLD system is not yet available for routine experimenter use.

2.2.2.2 Calcium Fluoride

Calcium fluoride TLDs (in chip form) are frequently used at NED when a quick readout of the exposure is desired. Results can be obtained within a few minutes after the TLDs are retrieved from the irradiation cell. The TLDs are unshielded and exhibit a strong energy dependence. Also, these dosimeters read 30% to 60% higher than LiF dosimeters when exposed to the same radiation environment at the FBR.

2.2.2.3 Gamma Dose Rate

Gamma dose-rate measurements were made with a Microsemiconductor Corporation MC-1546 computer diode. (This diode was recommended by personnel of the Autonetics Division of North American Rockwell.) A Solid State Radiations Incorporated PIN diode was also used to measure the gamma dose rate.

2.2.3 Results

2.2.3.1 Radial Measurements

Free-field gamma measurements with LiF TLDs were made by using the techniques outlined in paragraph 2.1.3.4. Gamma exposure per kilowatt-minute is plotted in Figure I-10. These measurements were made in the horizontal midplane of the core. Figure I-11 shows the gamma exposure as a function of distance from the core centerline for burst operations. The exposure is normalized to a 1-degree temperature rise in T_1.

2.2.3.2 Vertical Distribution

Figure I-12 shows the gamma exposure per ΔT_1 along a vertical traverse at 1 meter from the core centerline. The exposure was measured by LiF TLDs. The technique described in paragraph 2.1.3.5 was used to insure free-field conditions.

2. 2. 3. 3 Angular Dependence

The dependence of exposure on the angle with respect to north was deter-
mined by LiF TLDs. The TLDs were placed on the experimenter table,
which was positioned so that the surface of the table was in the midplane
of the core. The results of these measurements are shown in Figure I-13.

2. 2. 3. 4 Gamma Dose Rate

a. Gamma dose rate as a function of distance for both wide and nar-
row pulses is shown in Figure I-14. A Solid State Radiations Incorporated
PIN diode was used to measure the dose rate during the wide pulse (70 μsec
FWHM). Several bursts of the same yield were performed with the diode
positioned at different distances from the core. Three MC-1546 diodes
were used to measure the gamma dose rate as a function of distance from
the core centerline for a narrow pulse (40 μsec FWHM). In order to in-
sure that the three diodes had sensitivities that were essentially equal,
the diodes were exposed at the same distance from the core for two bursts.
The outputs were within ±5% of the mean of the three readings. The cali-
bration of these diodes was provided by personnel of Autonetics (Anaheim).

b. Gamma and neutron dose rates are approximately proportional to
the pulse height from a photodiode used to monitor the reactor pulse. A
burst picture or photograph of the photodiode oscilloscope trace is pro-
vided to the experimenter for each pulse. The reliability of this technique
is compromised by two effects of the high radiation fields:

(1) The darkening of the scintillator material

(2) The degradation of the photodiode due to neutrons

c. An alternate means of scaling dose rates depends on the ratio of
the peak fission rates for the two bursts in question. The peak fission
rate ($\dot{F}$) is given by (Ref 6)

$$\dot{F} = \frac{C a \rho}{2} (1 + a^2 \tau^2)$$

2-23

where C is the shutdown coefficient, a is the reciprocal of the initial period in seconds, ρ is the prompt reactivity, and τ is the characteristic propagation time of pressure waves in the assembly. The period appears on the burst photograph, the prompt reactivity can be obtained from reactor performance data, and t is approximately 12 microseconds. For the bursts in Figure I-14, the calculated ratio is

$$\frac{\dot{F}_1}{\dot{F}_2} = 1.79$$

Here, $\dot{F}_1$ and $\dot{F}_2$ are the peak fission rates for the 40- and 70-microsecond pulses, respectively. The corresponding ratio obtained from the measured dose rates is 1.5.

2.3 OPERATING LIMITS AND FACTORS AFFECTING FBR OUTPUT CHARACTERISTICS

2.3.1 Objective

The objective of this section is to provide the user of the facility with a summary of operating limits and factors affecting the output characteristics of the FBR.

2.3.2 Method

The information in this section is based on documented administrative limits and on FBR operating experience.

2.3.3 Results

2.3.3.1 Effects of Moderating Materials

a. There are no materials of low atomic weight in the FBR core to effectively moderate the neutrons produced in fission. The vast majority of fissions, therefore, are produced by high-energy neutrons. It is the absence of moderating material and the compact construction of the core that account for the very short neutron lifetime, the narrow pulsewidths, and the high dose rates produced by the FBR. The fact that it is a bare, unmoderated, and highly enriched assembly makes the reactor extremely sensitive to the moderating and reflecting characteristics of experiments placed near it (Ref 12 and 13). A decoupling shroud or "safety shield" lined with cadmium is used to reduce the effects of external reflectors by absorbing and scattering thermal neutrons which are reflected back toward the core. The decoupling provided by the cadmium is not complete, and experiments (especially moderating experiments) broaden the pulse and reduce the dose rates produced by a burst of a given yield. Figure 5 shows two bursts of approximately the same yield, but the pulsewidth, and consequently the peak dose rate, is altered drastically because moderating material was placed near the core.

2-25

Figure 5 Comparison of burst profiles between unreflected and moderated bursts.

① - Unreflected

② - Moderated, polyethylene reflector (1 ft - cube) reflector at 6" ℄.
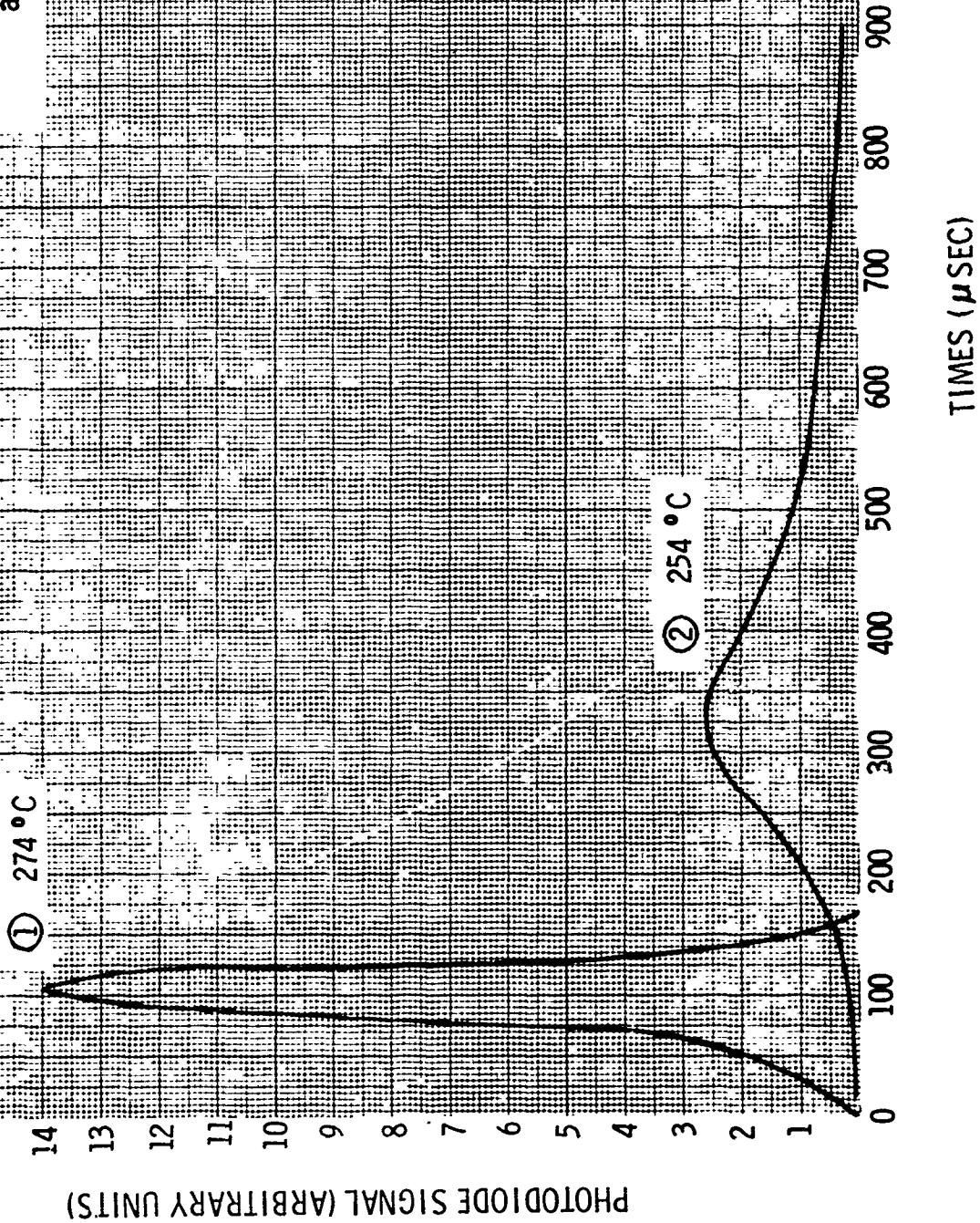
① 274 °C

② 254 °C

PHOTODIODE SIGNAL (ARBITRARY UNITS)

TIMES (μSEC)

b. The effects of moderating material on the burst yield are illustrated in Figure 6. The moderating experiment setup consisted of two 4- by 8- by 2-inch polyethylene bricks placed on the experimenter table so that the 8- by 8-inch surface formed by the two bricks was perpendicular to a core radius. The distance plotted is measured from the core centerline to the surface of the reflector. Figure 6 shows a very strong effect on the burst yield. This effect can be reduced somewhat by placing additional cadmium between the reflector and the core. The boron-10 decoupling shroud (para 1.2) will essentially eliminate this effect (Ref 14 and 15).

2.3.3.2 Position Relative
          to the Burst Rod

a. As shown in Figure 1, the burst rod is inserted at a location near the external surface of the reactor. For this reason, its reactivity worth is affected by the presence of external reflectors placed near it. The experiment reflects neutrons back into the core and is capable of tilting the flux distribution sufficiently to alter the burst rod worth. The burst rod is inserted at a position that is 30 degrees from north and at a radius of 3.125 inches from the core axis of symmetry.

b. The dependence of burst yield on the angular position of a reflector can best be analyzed by comparison with the effects of a symmetric reflector with the same moderating characteristics as the reflector in question. Experiments placed between 90 and 270 degrees with respect to the burst rod tend to reduce the yield of a burst, while those between 270 and 90 degrees tend to increase the burst yield (Fig. 7) relative to those produced with a symmetric experiment.

c. Figure 8 shows the effect of the angular position of an 8- by 8- by 1-inch steel plate on the burst yield. The 8- by 8-inch face was kept perpendicular to a radius; the distance to the core centerline was 6 inches. This curve shows the very strong dependence of burst yield on angular position.
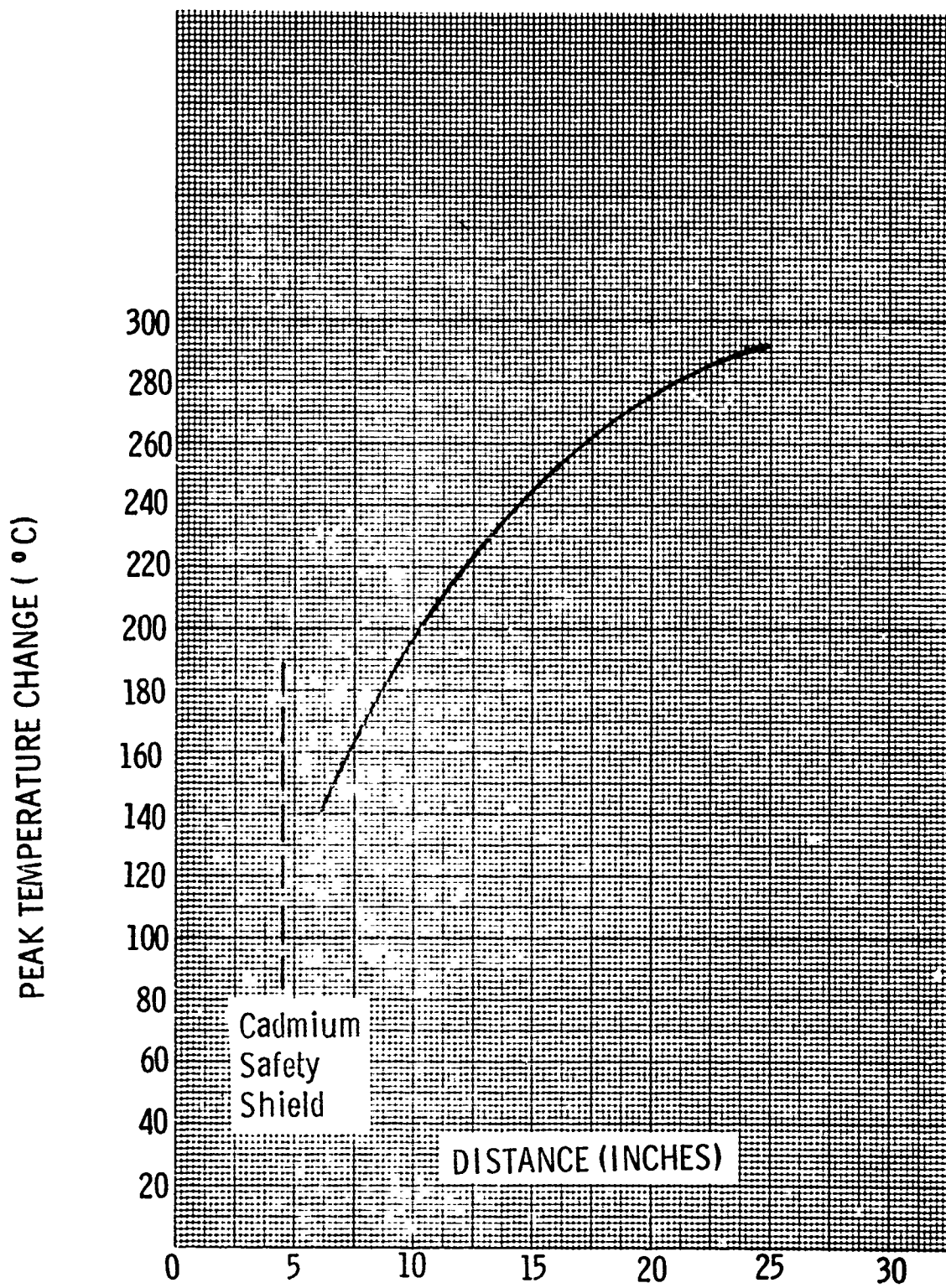
Figure 6   Temperature yield vs. radial distance
            from core centerline as determined
            with a moderating experiment.

N

←30°→

Experiments which
tend to add reactivity
worth to the burst rod

Experiments which
tend to reduce the
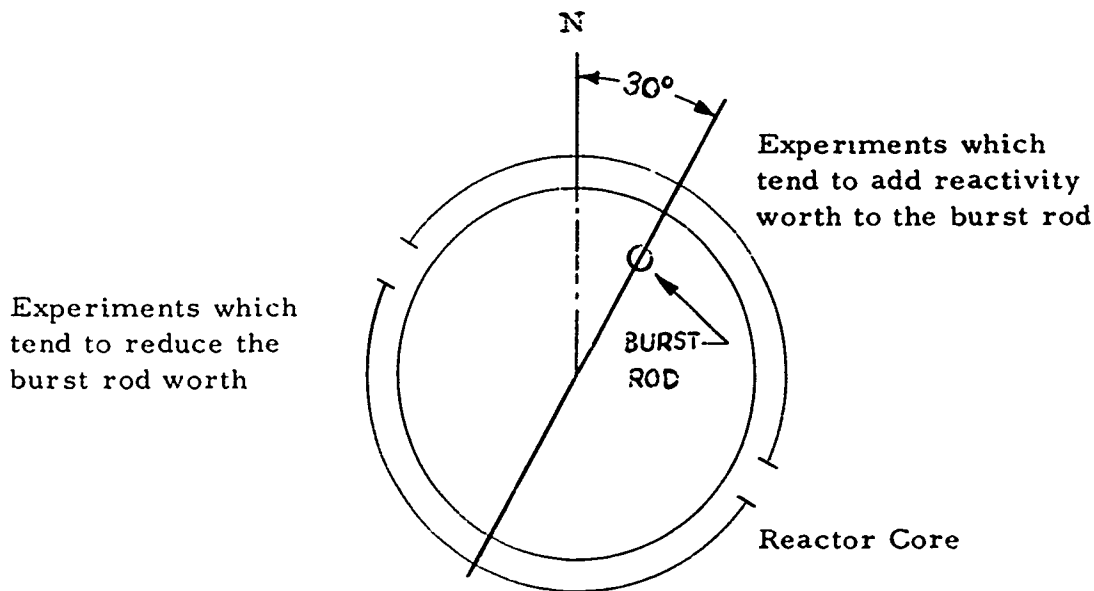burst rod worth

BURST
ROD

Reactor Core

Fig. 7.   Location of Experiments With Respect to the Burst Rod

d.   Generally, experiments are positioned so that they tend to
reduce the burst yield. If this is done, initial burst operations smaller
than the desired yield are obtained for new types of experiments or
those of high experimental worth by compensating for the experiment as
though it were symmetrically distributed around the core. After the
characteristics of the new experiment are determined, bursts of the
desired yield can be produced consistently. This technique enables the
Reactor Leader to approach the burst of the desired size from the con-
servative direction.

2. 3. 3. 3 Limitations on
           Experimental Worth

a.   The size and moderating characteristics of the experiment and
its proximity to the core are critical factors in determining its effect
on the FBR. It is possible for the worth of an experiment to exceed the
amount of reactivity that can be withdrawn with the control rods. In
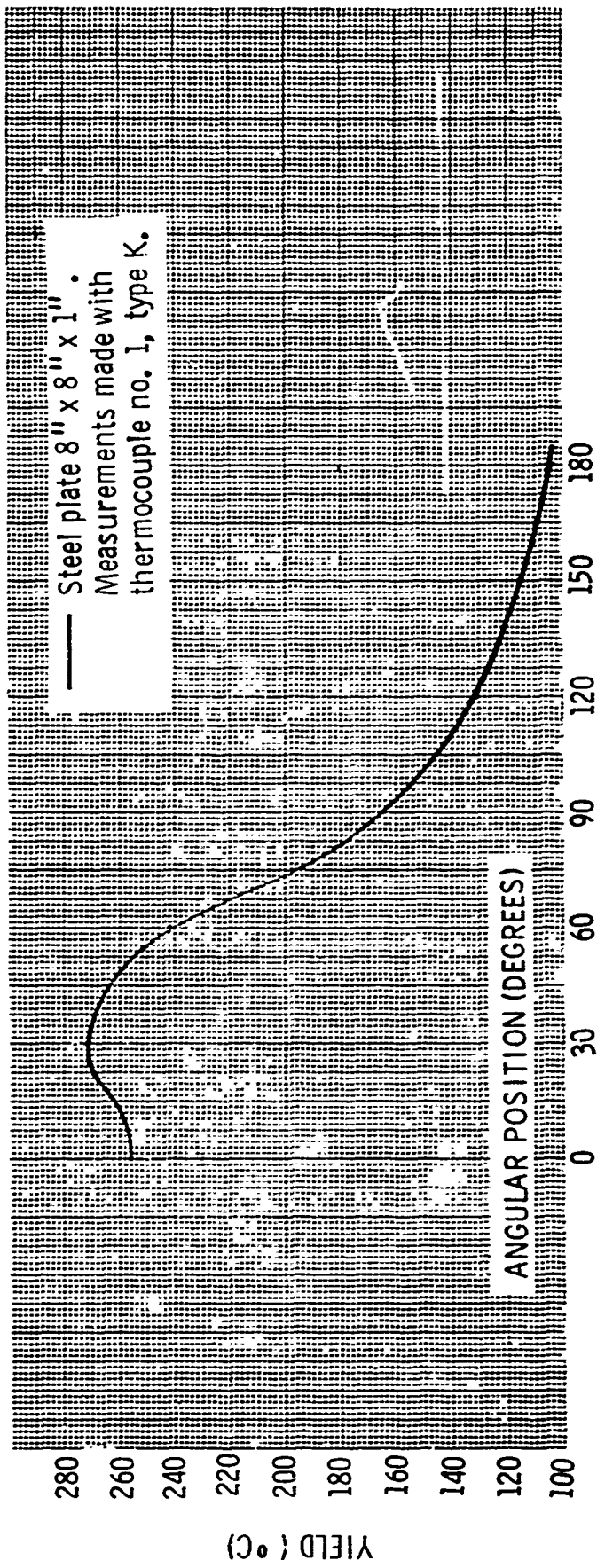order to maintain shim capability in the control rods and to limit the

Figure 8   Maximum temperature yield as a function
of angular position for a steel plate at
6 inches from core centerline.

2 - 3

effects of experiments on the burst yield, a limit is placed on experimental worth. This reactivity limit is $1.50 relative to the unreflected reactor with no experiment table in proximity to the core. Experiments exceeding this limit can be irradiated only with the concurrence of the Reactor Safeguards Committee (RSC).

b. The mass adjustment ring (MAR) is removed from the core when experiments exceeding $1.50 are exposed. The removal of the hollow stainless-steel MAR provides an additional $0.62 of shim adjustment. The reactivity worths of other core components are listed in Table VIII.

TABLE VIII

REACTIVITY WORTHS OF CORE COMPONENTS

Component		Worth ($)
Burst Rod		1.11
Hollow Stainless-Steel MAR		0.62
Solid Stainless-Steel MAR		1.04
U—10 wt. % Mo MAR		2.46
Safety Block, $\frac{1}{2}$ inch		1.42
Safety Block, 1 inch		3.77
Safety Block, $1\frac{1}{2}$ inches		>4.92
Control Rod (peak differential)	No. 1	0.0365 (¢/mil)
	No. 2	0.0345 (¢/mil)
Control Rod (integral)	No. 1	1.59
	No. 2	1.54

c. The analytical evaluation of the reactivity worth of an experiment is a complex problem involving the energy-dependent scattering and absorption cross sections of all the materials involved, the solid angle these materials subtend, and their density, thickness, etc. Because of the complexity of the problem of estimating the worth of an experiment a priori, it is recommended that large experiments that must be placed very close to the reactor be designed so that their reactivity can be reduced. This can be done by segmentation of the experiment or by moving the experiment back. The reactivity contribution of an experiment falls off more rapidly than $1/R^2$, so a small change in its position is generally sufficient to reduce its worth to a value of less than $1.50.

2.3.3.4 Limitations and Predictability
        of Burst Operations

a. Experimenters typically request exposures requiring bursts in the range between 210° and 270°C. The maximum yield allowable without prior approval of the RSC is $\Delta T_3 = 300°C$ ($\Delta T_1 = 355°C$). For narrow bursts greater than about $\Delta T_1 = 310°C$, the probability of minor mechanical failures that could delay operations increases. In addition, health physics problems become more complex. The flaking of the nickel fuel cladding is accelerated because of the increased thermal shock. Traces of fuel cladding and fission products on the reactor cell floor force the implementation of special procedures to prevent the spread of contamination. The replating of core components with aluminum ion plating has reduced the problem somewhat: however, the problems of contamination associated with larger bursts have not been eliminated.

b. The checkout of the modified core, which is part of a development program to improve reactor operational capability, will provide information for the identification and elimination of structurally weak points in the FBR system As a result of the core modification, the limit on burst yield will be raised to the vicinity of $\Delta T_1 = 400°C$.

c.   When new experiments are set up near the core, the Reactor
Leader approaches the desired yield rapidly through a series of bursts
if the experimental setup is not altered greatly from burst to burst.
Under the ideal conditions, in which the experiment is not changed, the
yield can be expected to vary less than ±5%.   On the order of 2% of the
time, neutrons from spontaneous fissions, fissions produced directly or
indirectly by cosmic rays, or those produced by delayed neutrons cause
a power excursion before the burst rod is fully seated.   These preinitia-
tions result in yields which may be as small as 20% of the desired burst
yield.

2. 3. 3. 5 Limitations on
          Power Operations

a.   Power operations can be run for several hours at levels from
fractions of watts to 5 kilowatts and for short periods of time up to about
10 kilowatts.   (A 10-kilowatt power level can be maintained for approxi-
mately 10 minutes.) The limiting factor in power operations is the limit
of 400°C maximum core temperature stated in the FBR Technical
Specifications (Ref 16).   An improved forced-air or a liquid nitrogen cool-
ing system would permit operation at higher power levels.   Figure I-15
shows the reactor core temperature (T_1) as a function of time for various
power levels.   The T_1 temperature scram point is set at 350°C, and with
the cooling system in operation, it can be seen that 5 kilowatts is very
close to the maximum power level that can be maintained indefinitely.

b.   For the FBR, the buildup of fission products may restrict main-
tenance operations necessary for continued pulse operation.   The number
of fissions normally produced by one full day of burst operations (5 bursts,
5×10^{17} fissions) are produced by the FBR running at 5 kilowatts for about
1 hour.   For this reason, long power runs must be carefully scheduled so
that the high radiation levels produced by the decay of fission products do
not limit reactor maintenance operations.

2-33

SECTION 3. APPENDICES
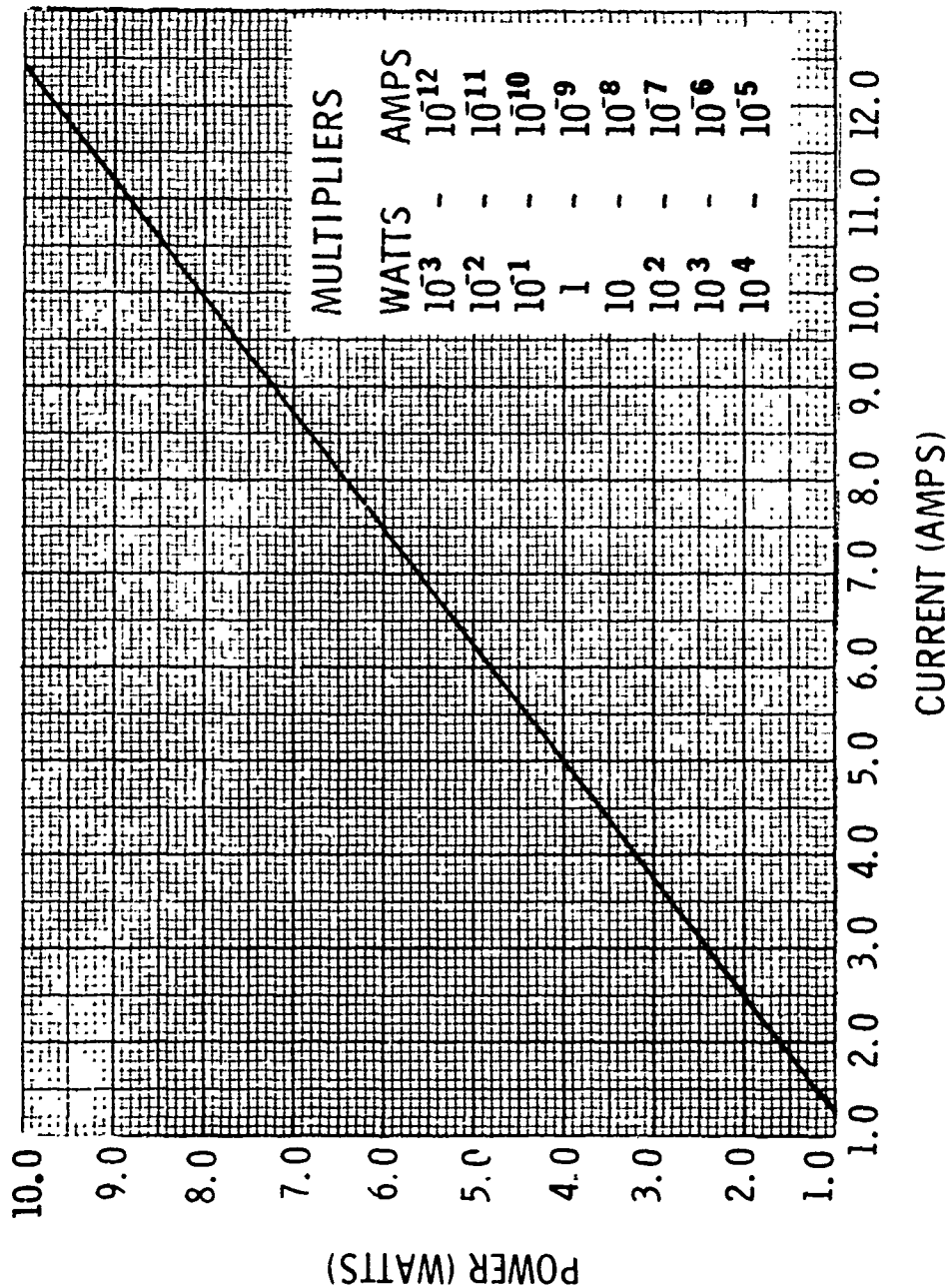
APPENDIX I.   TEST DATA

Figure I-1   Steady state reactor power vs. current as determined from compensated ionization chamber. (channel no. 1)
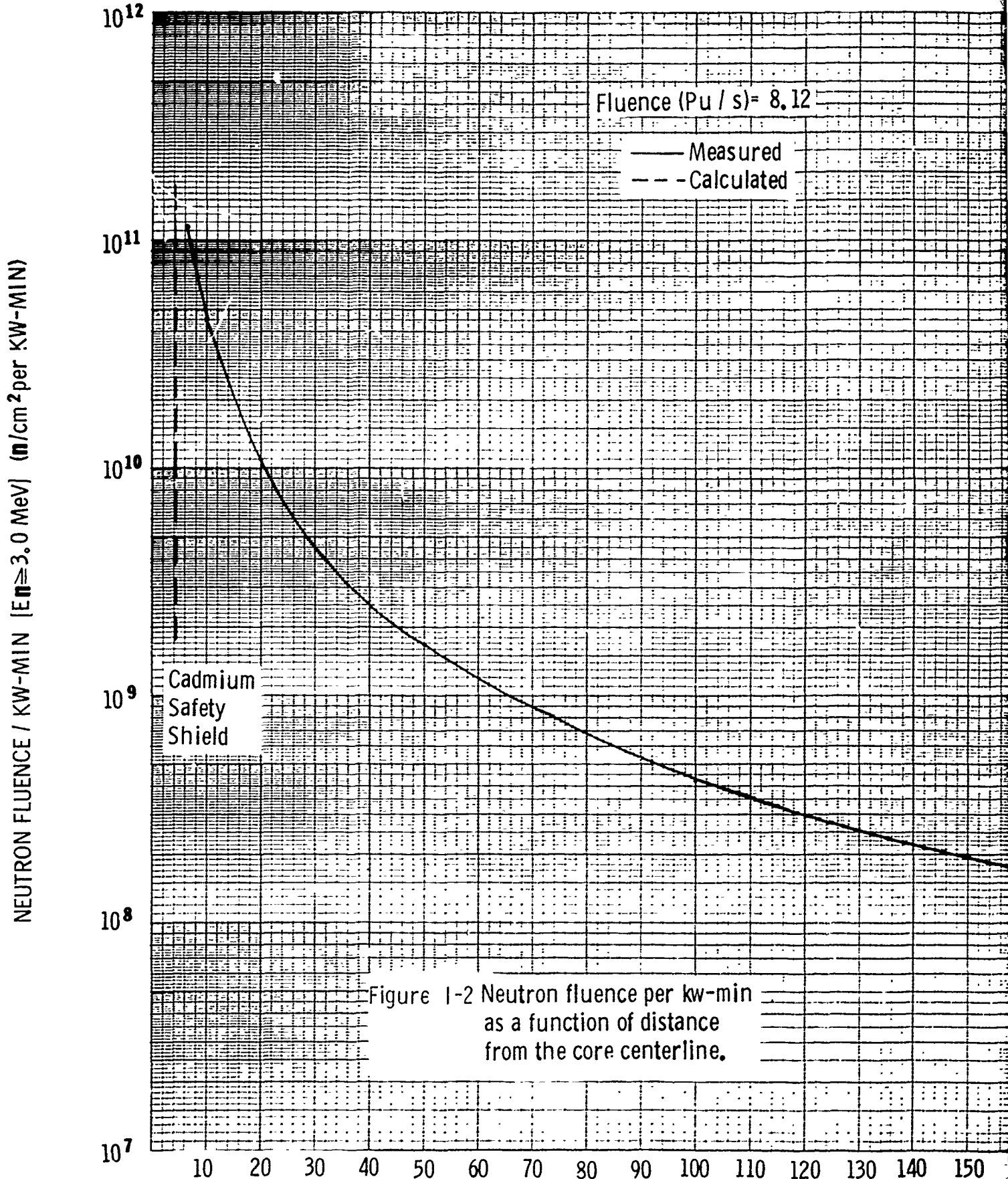
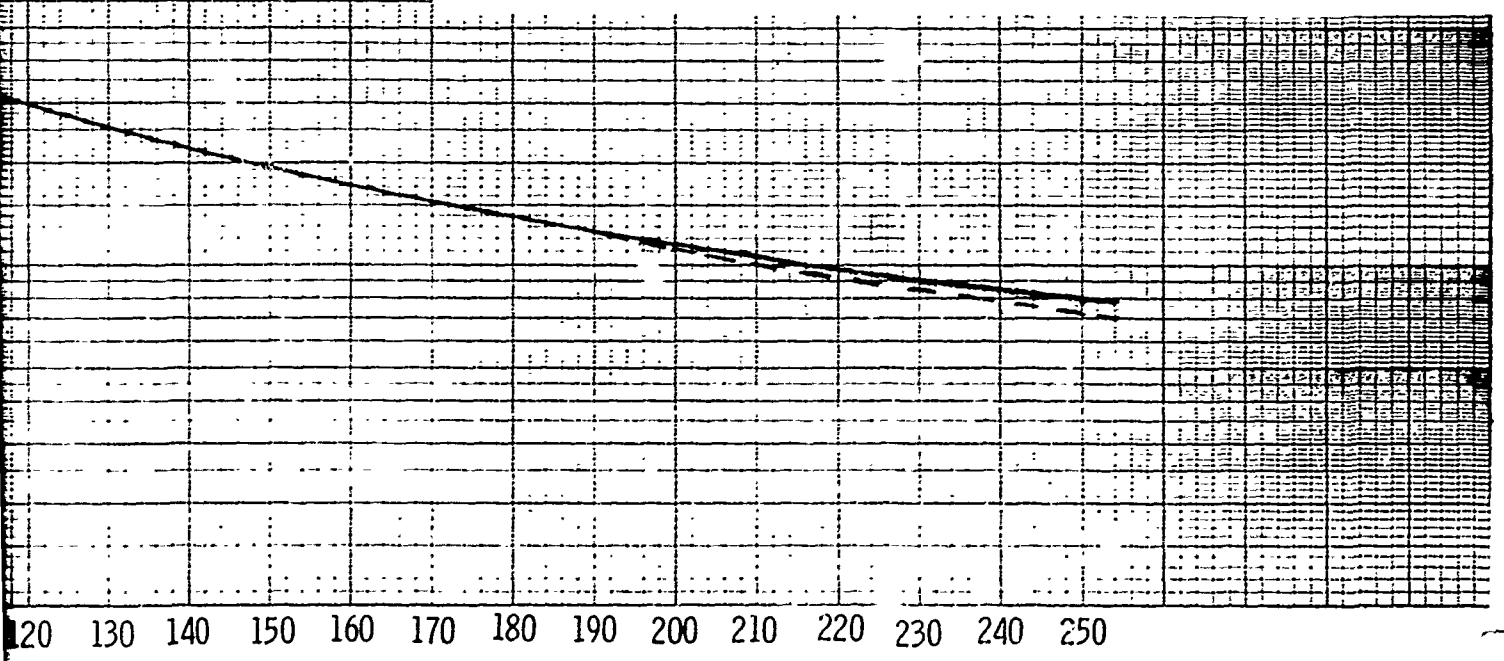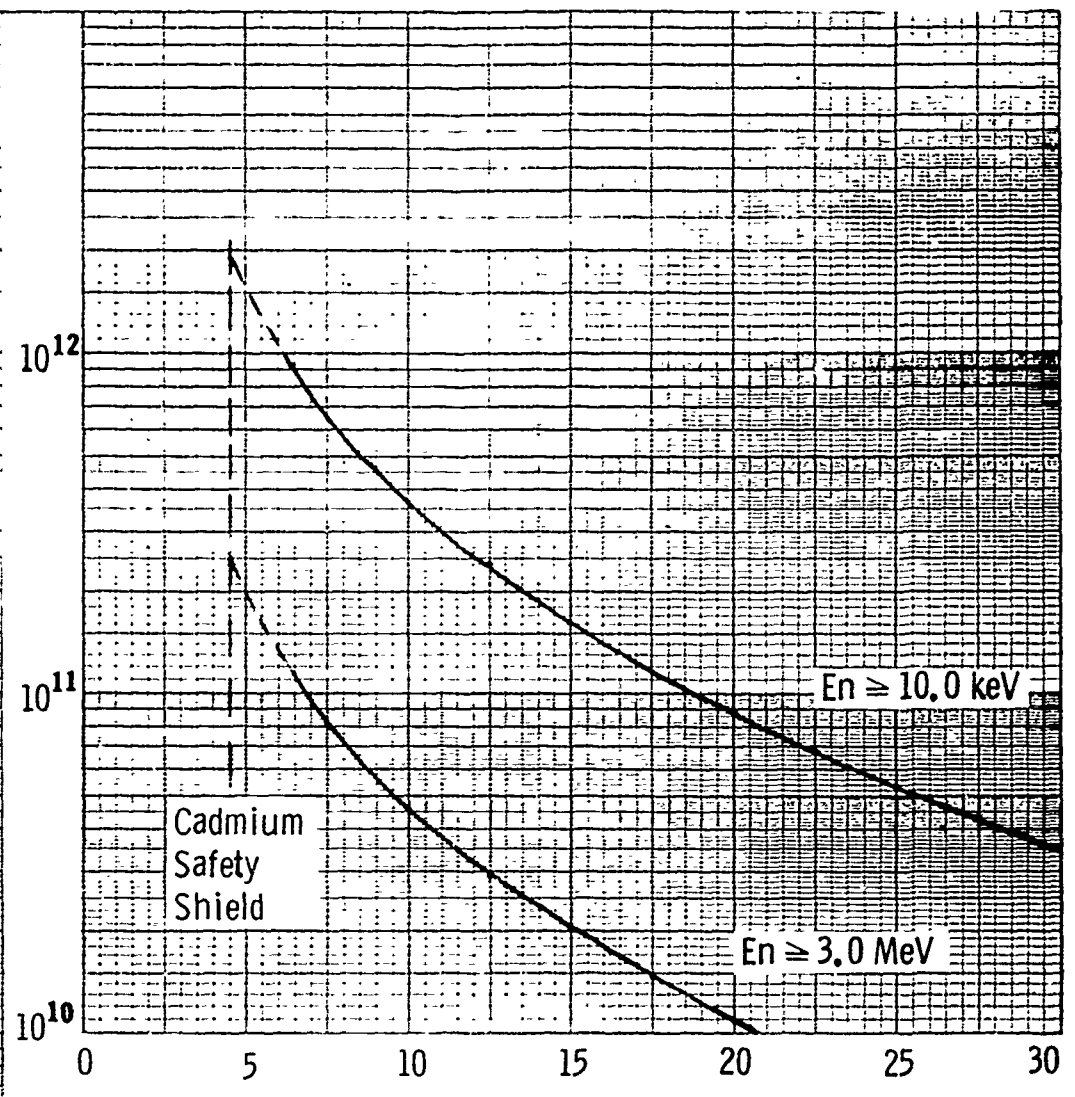Figure I-2 Neutron fluence per kw-min as a function of distance from the core centerline.

Fluence (Pu / s)= 8.12

—— Measured
— — -Calculated

Cadmium Safety Shield

NEUTRON FLUENCE / KW-MIN [En ≧ 3.0 MeV] (n/cm² per KW-MIN)

DISTANCE FROM REACTOR CORE CENTER

.12

10^{12}

10^{11}

En ≥ 10.0 keV

Cadmium
Safety
Shield

En ≥ 3.0 MeV

10^{10}

0   5   10   15   20   25   30

120 130 140 150 160 170 180 190 200 210 220 230 240 250

EACTOR CORE CENTERLINE (INCHES)

2
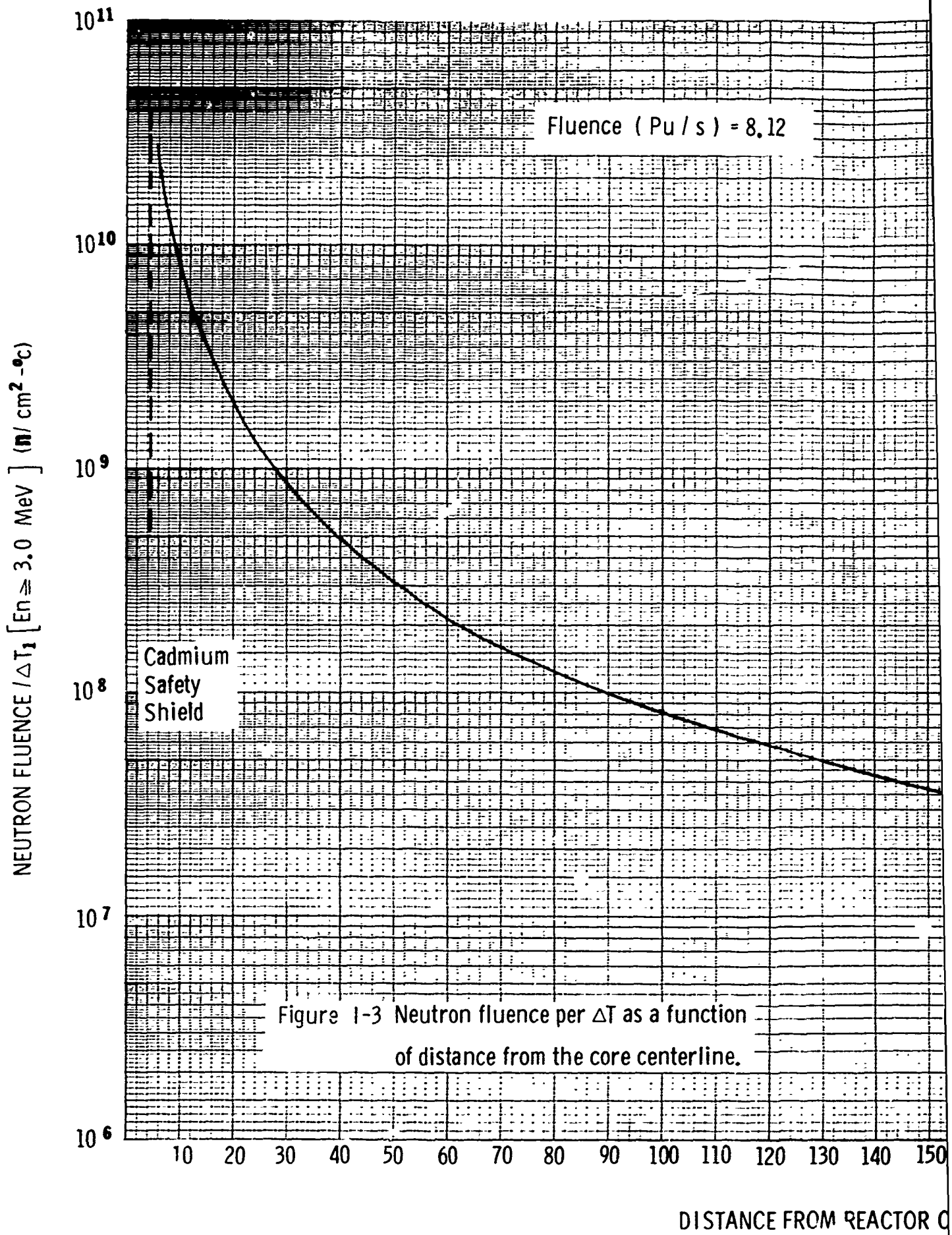
Figure 1-3 Neutron fluence per ΔT as a function of distance from the core centerline.

Fluence (Pu / s) = 8.12

Cadmium Safety Shield

NEUTRON FLUENCE / $\Delta T_1 \left[En \geqq 3.0 \text{ MeV} \right]$ ($n / cm^2 - {}^\circ c$)

DISTANCE FROM REACTOR C

En ≥ 10.0 keV

En ≥ 3.0 MeV

Cadmium Safety Shield

10^{11}

10^{10}

10^{9}

5   10   15   20   25   30

Measurements made with thermocouple no. 1, type K.

130   140   150   160   170   180   190   200   210   220   230   240   250   260   270   280   290   300
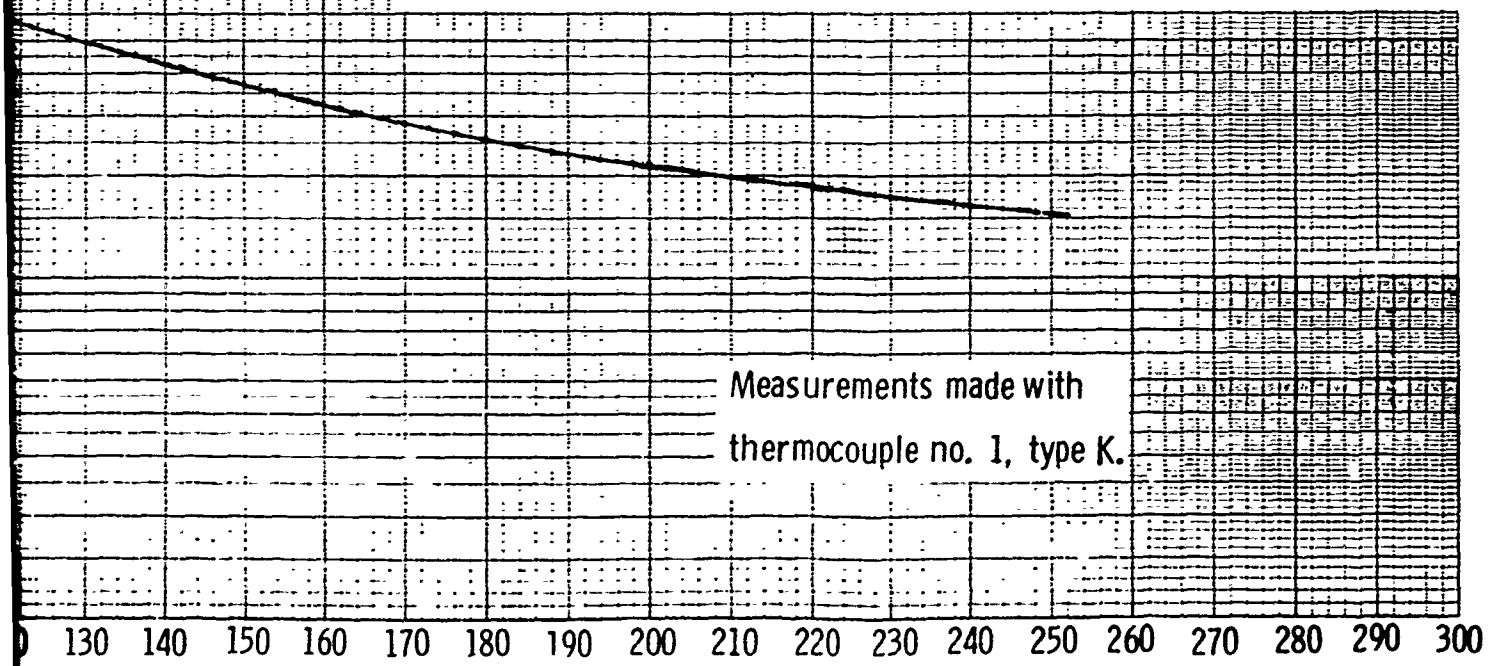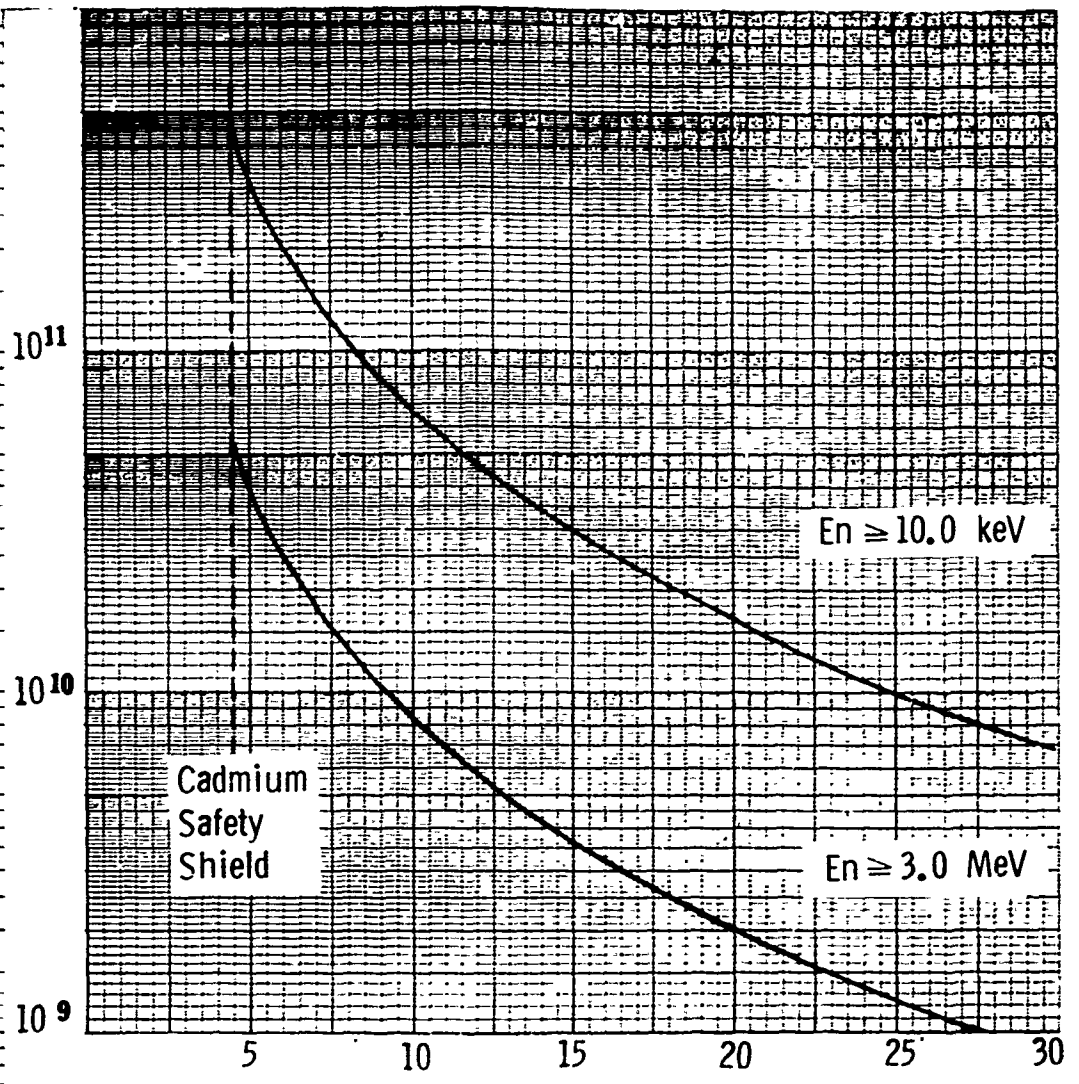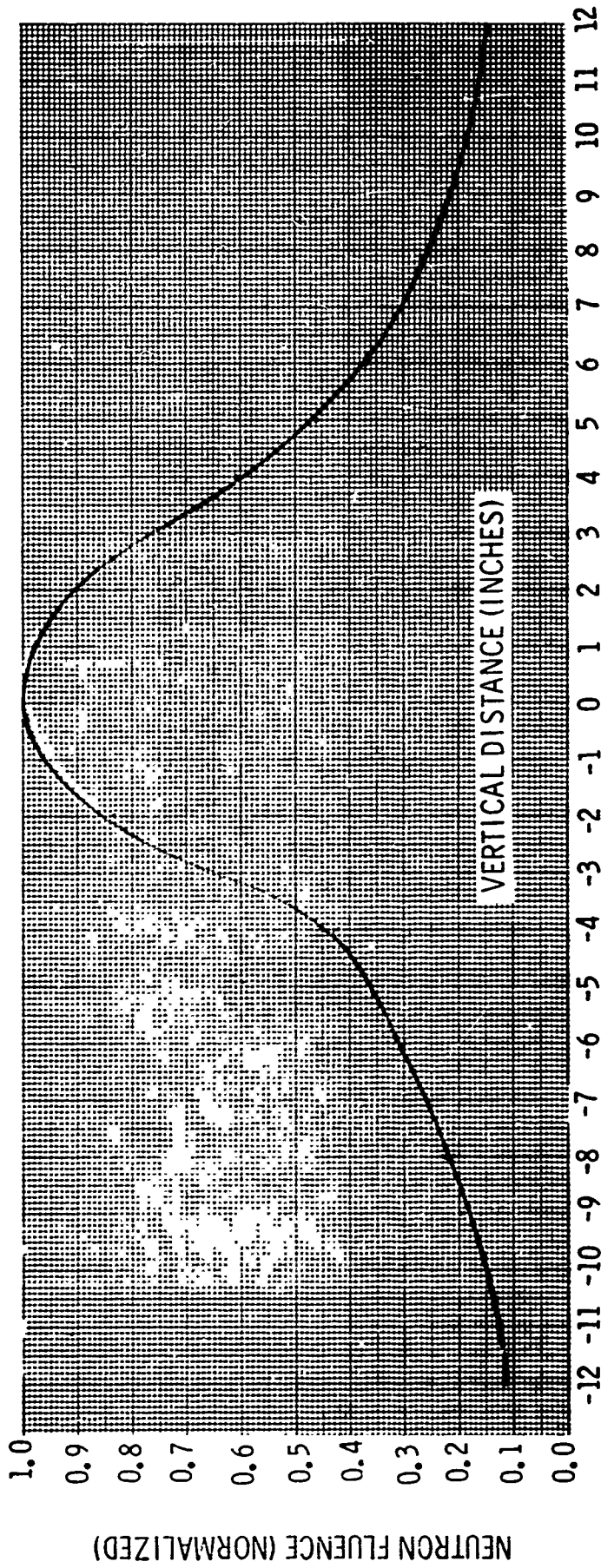
FROM REACTOR CORE CENTERLINE

2

Figure 1-4 Relative neutron fluence as a function of vertical distance from core midplane at 6 inches from core centerline. (Measured with experiment table.)
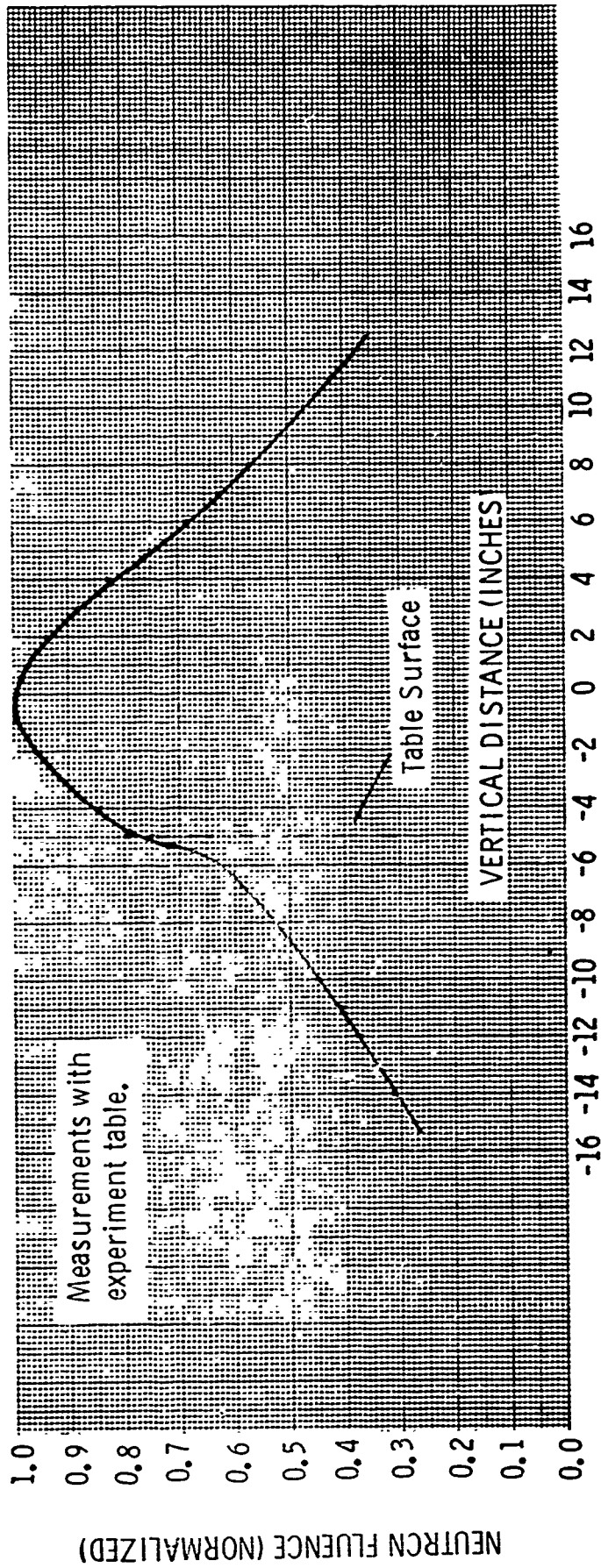
Figure 1-5 Relative neutron fluence as a function of vertical distance from core midplane at 12 inches from core centerline.

NEUTRON FLUENCE (NORMALIZED)

VERTICAL DISTANCE (INCHES)

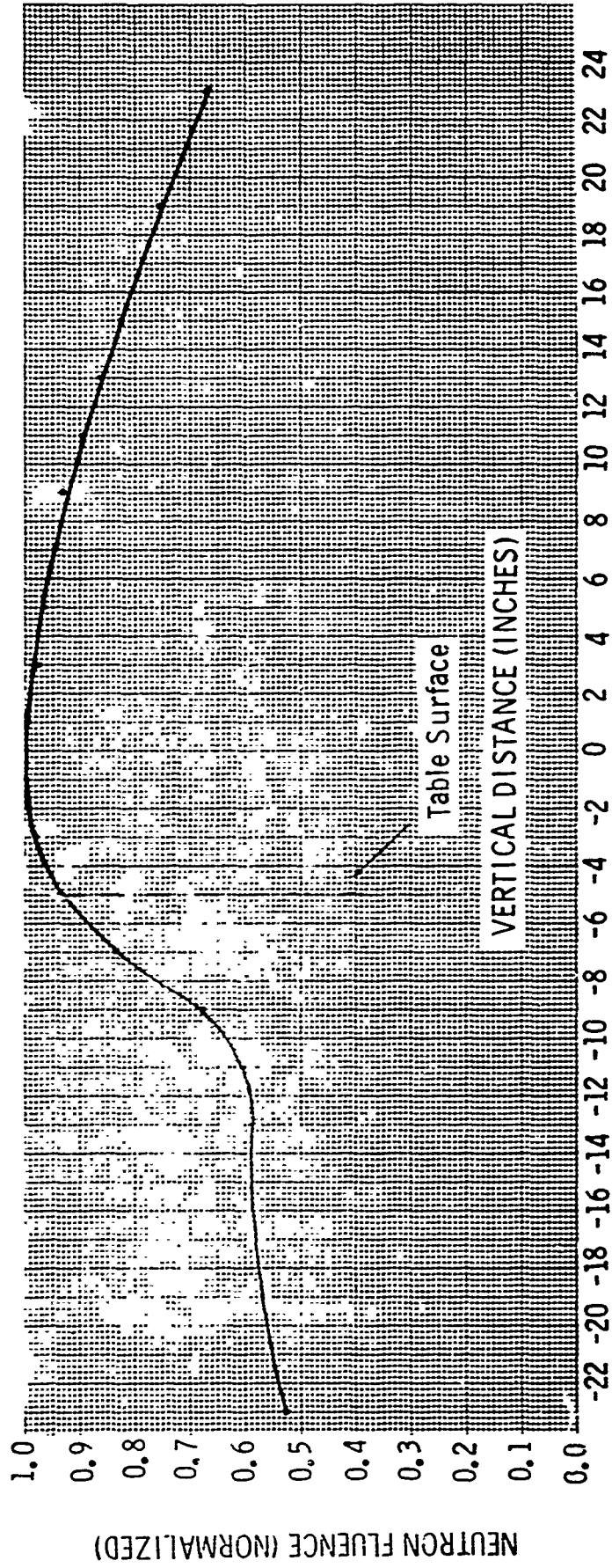Measurements with experiment table.

Table Surface

Figure 1-6 Relative neutron fluence as a function of vertical distance from core midplane at one meter from core centerline. (Measured with experiment table.)

NEUTRON FLUENCE (NORMALIZED)

VERTICAL DISTANCE (INCHES)

Table Surface
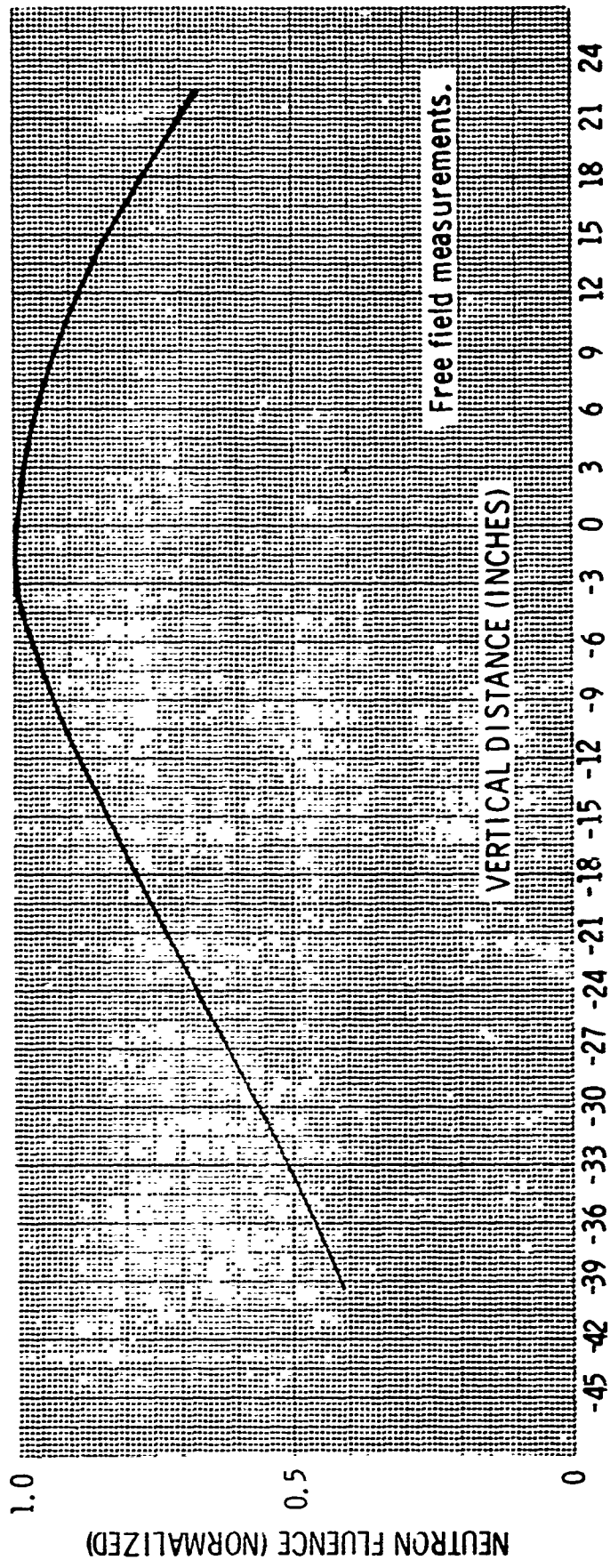
Figure 1-7 Relative neutron fluence as a function
of vertical distance from core midplane
at one meter from core centerline.

Figure I - 8. Neutron fluence as a function of angle at several distances. (Measured at core midplane.)

FLUENCE (Neutrons/CM²)

ROTATIONAL POSITION (Degrees)

Safety Shield (4.5")

6 inches

7 inches

8 inches

9 inches

10 inches

I-11
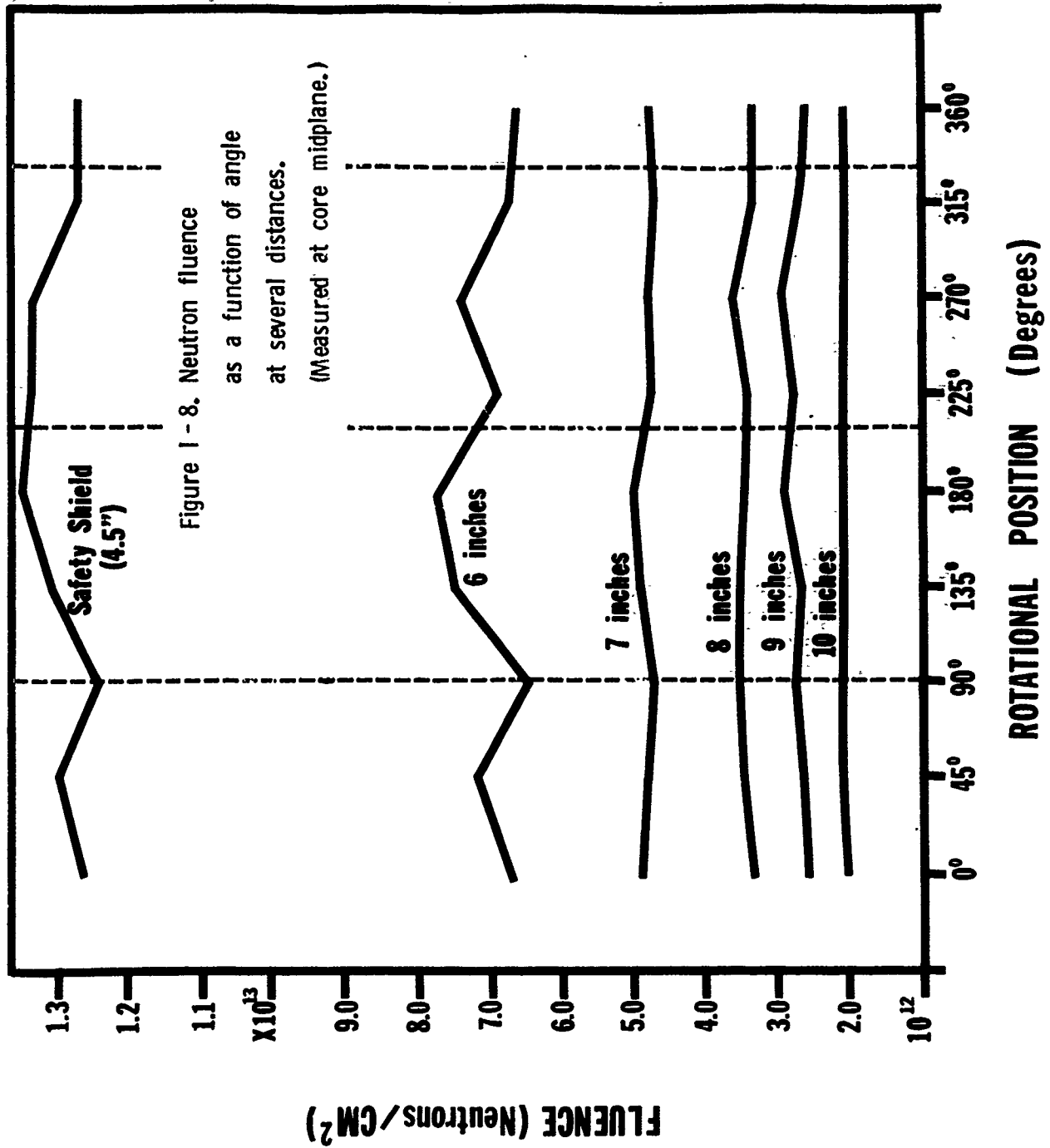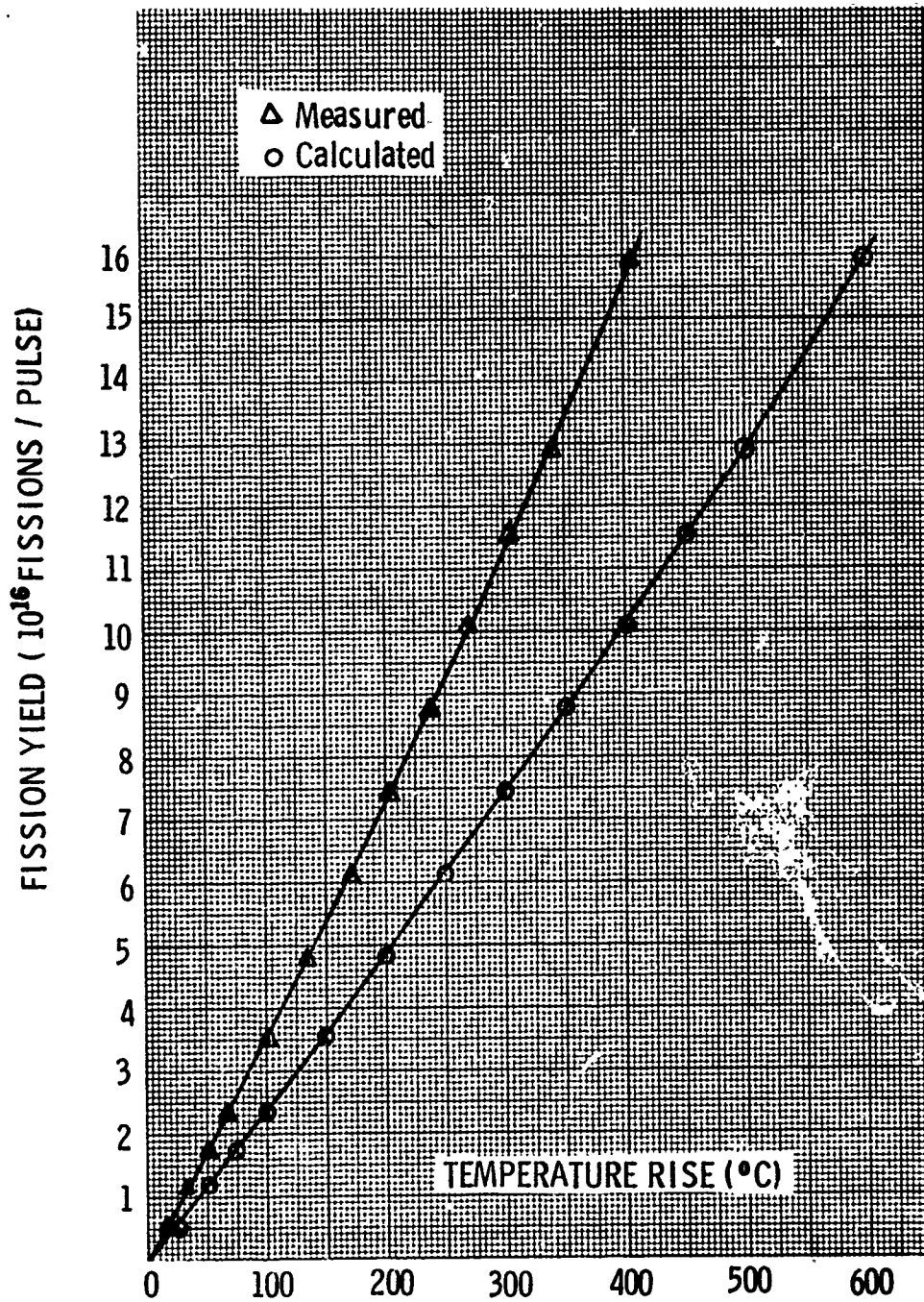
Figure I-9 Fission yield vs temperature rise (TC-1).
96.5 kg core
Temperature (Peak / Avg) = 2.08
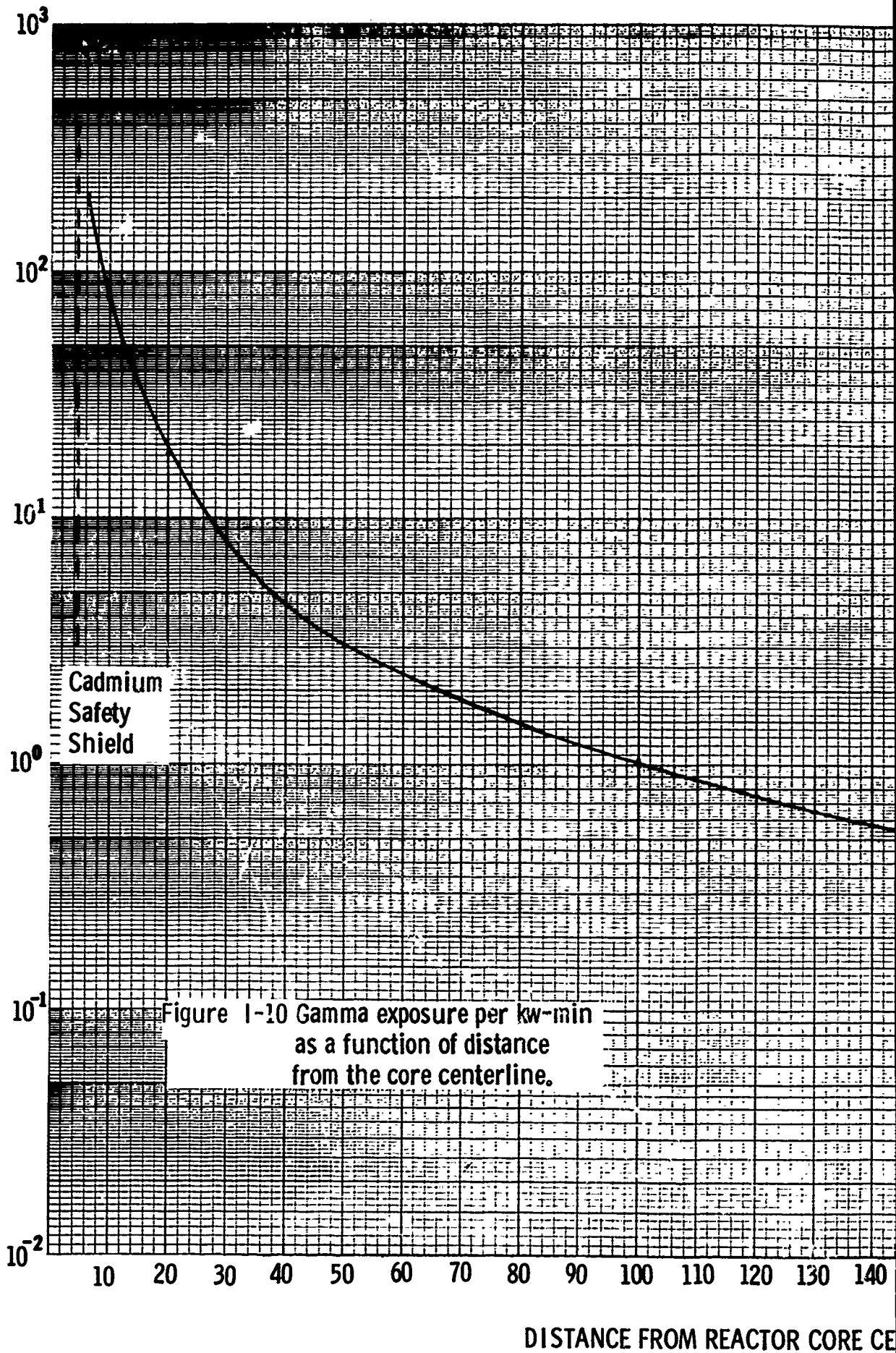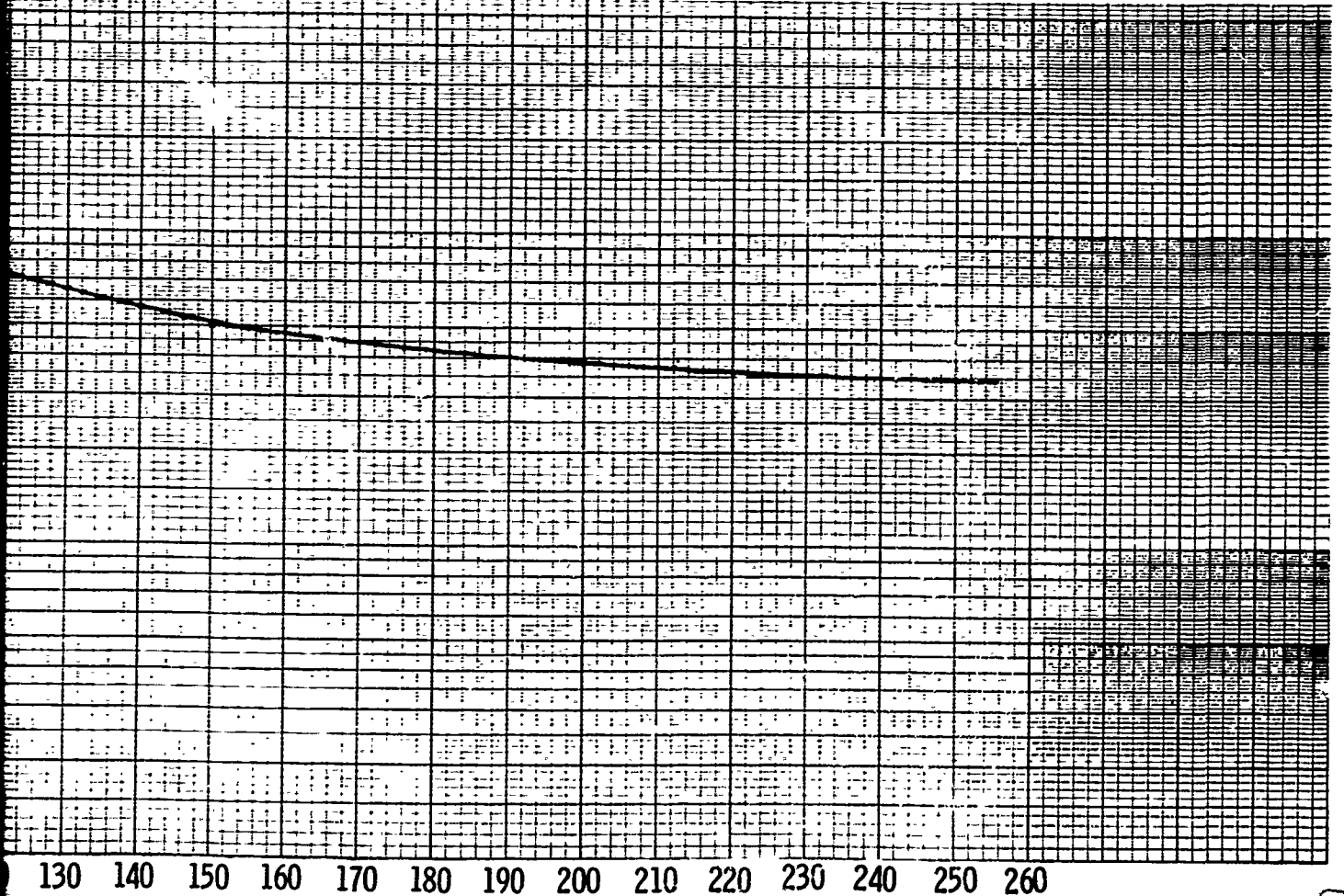
Figure I-10 Gamma exposure per kw-min as a function of distance from the core centerline.

DISTANCE FROM REACTOR CORE CE

Cadmium
Safety
Shield

10^3

10^2

10^1

0   5   10   15   20

130 140 150 160 170 180 190 200 210 220 230 240 250 260

OR CORE CENTERLINE (INCHES)

Figure 1-11 Gamma exposure per ΔT as a function of distance from the core centerline.

GAMMA EXPOSURE / ΔT (R / °C)

Cadmium
Safety
Shield

DISTANCE FROM REA

Pages I-15 and I-16

as a function
centerline.

Cadmium
Safety
Shield

10^2

10^1

10^0

0   5   10   15   20
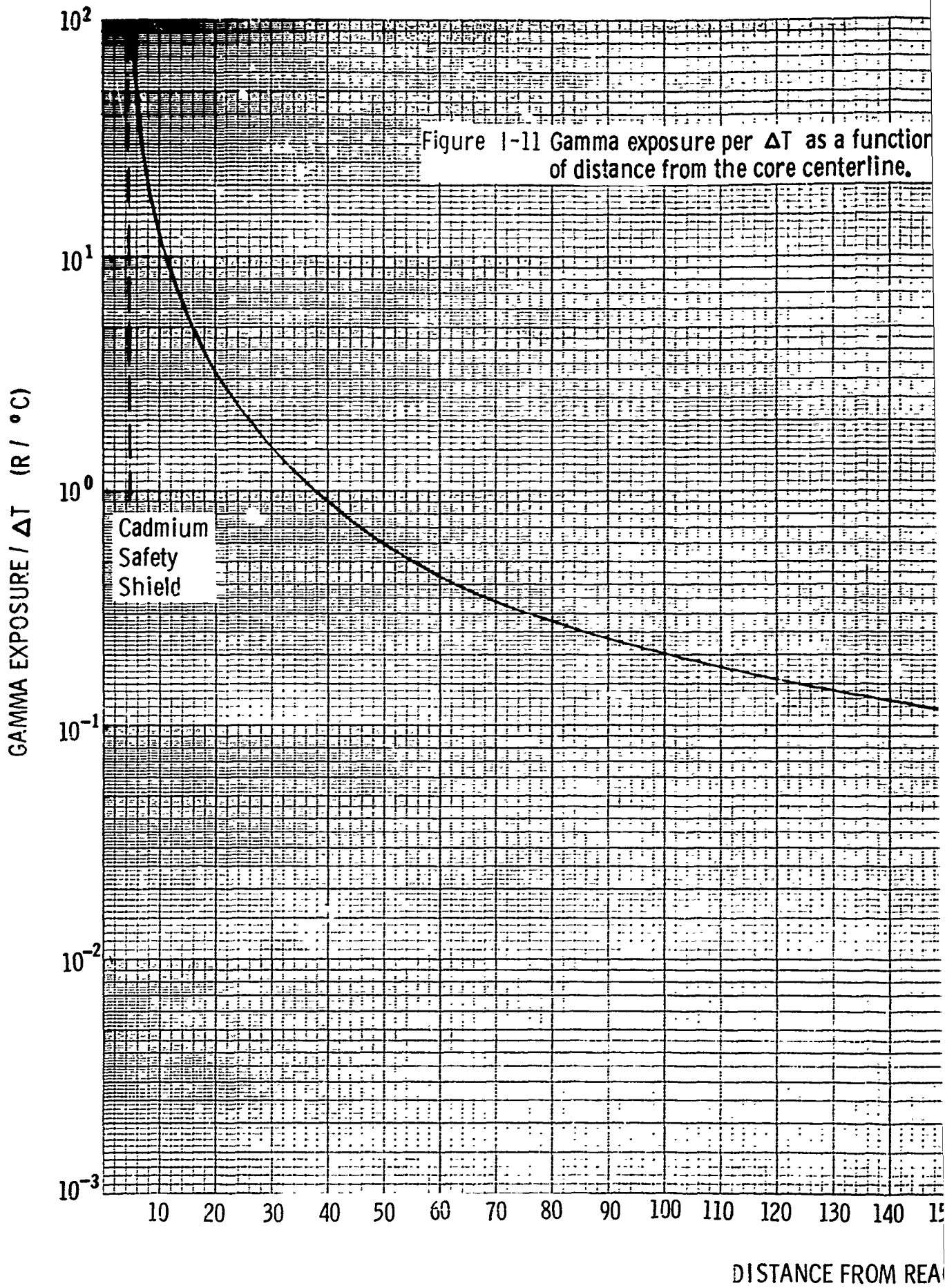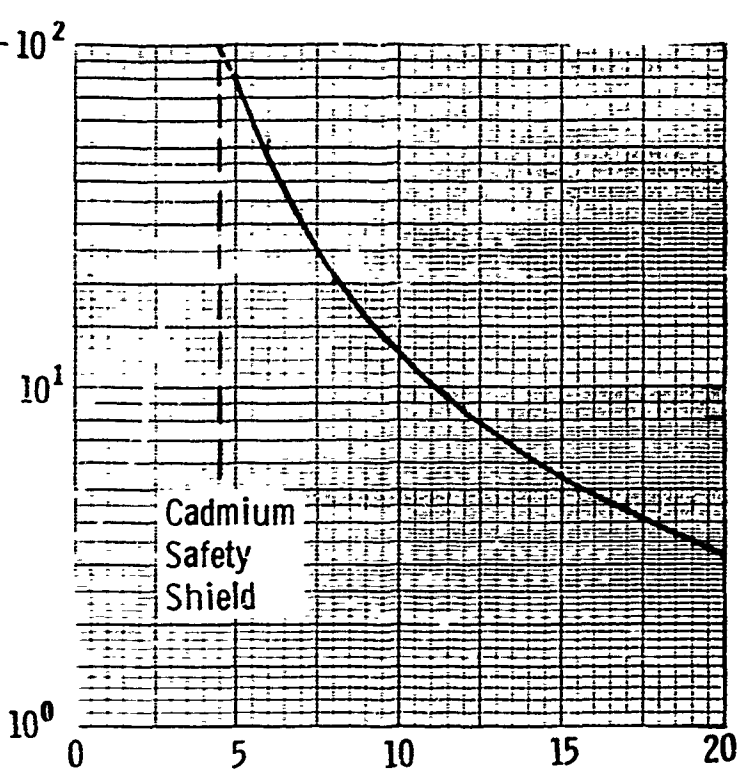
Measurements made with
thermocouple no. 1, type k.

130 140 150 160 170 180 190 200 210 220 230 240 250 260 270 280 290 300

2
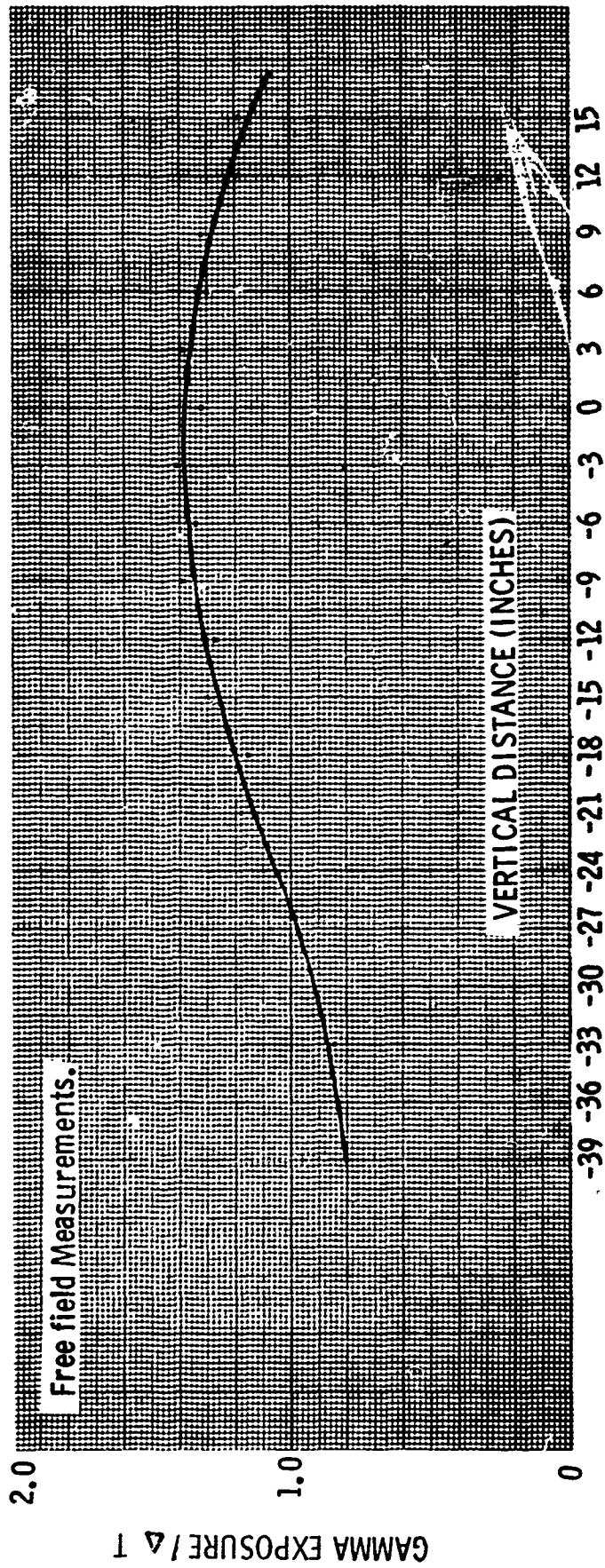
Figure 1-12 Gamma exposure/ ΔT as a function of vertical distance from core midplane at one meter from core centerline.

Figure I-13   Gamma exposure as a function
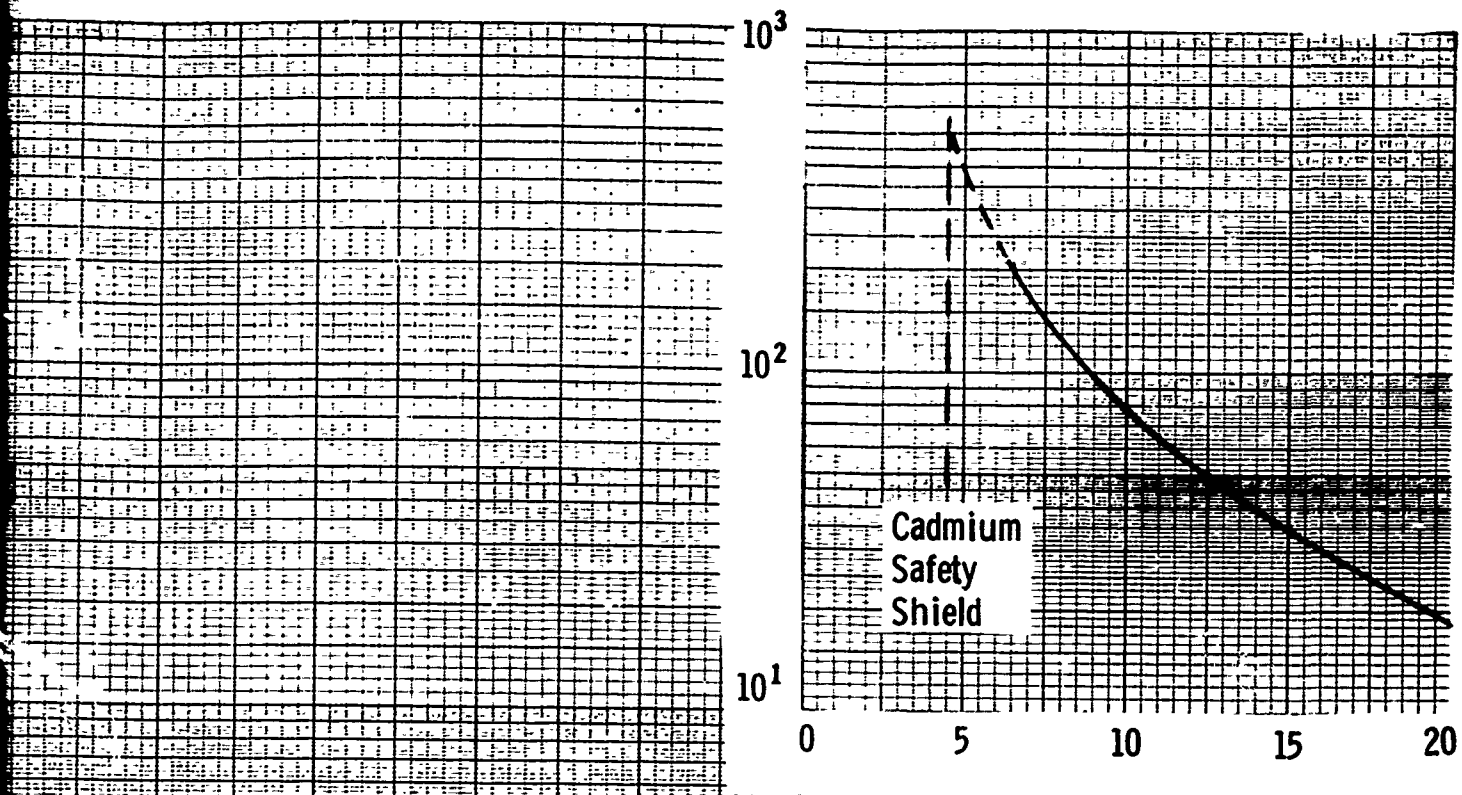of angle, at core midplane.
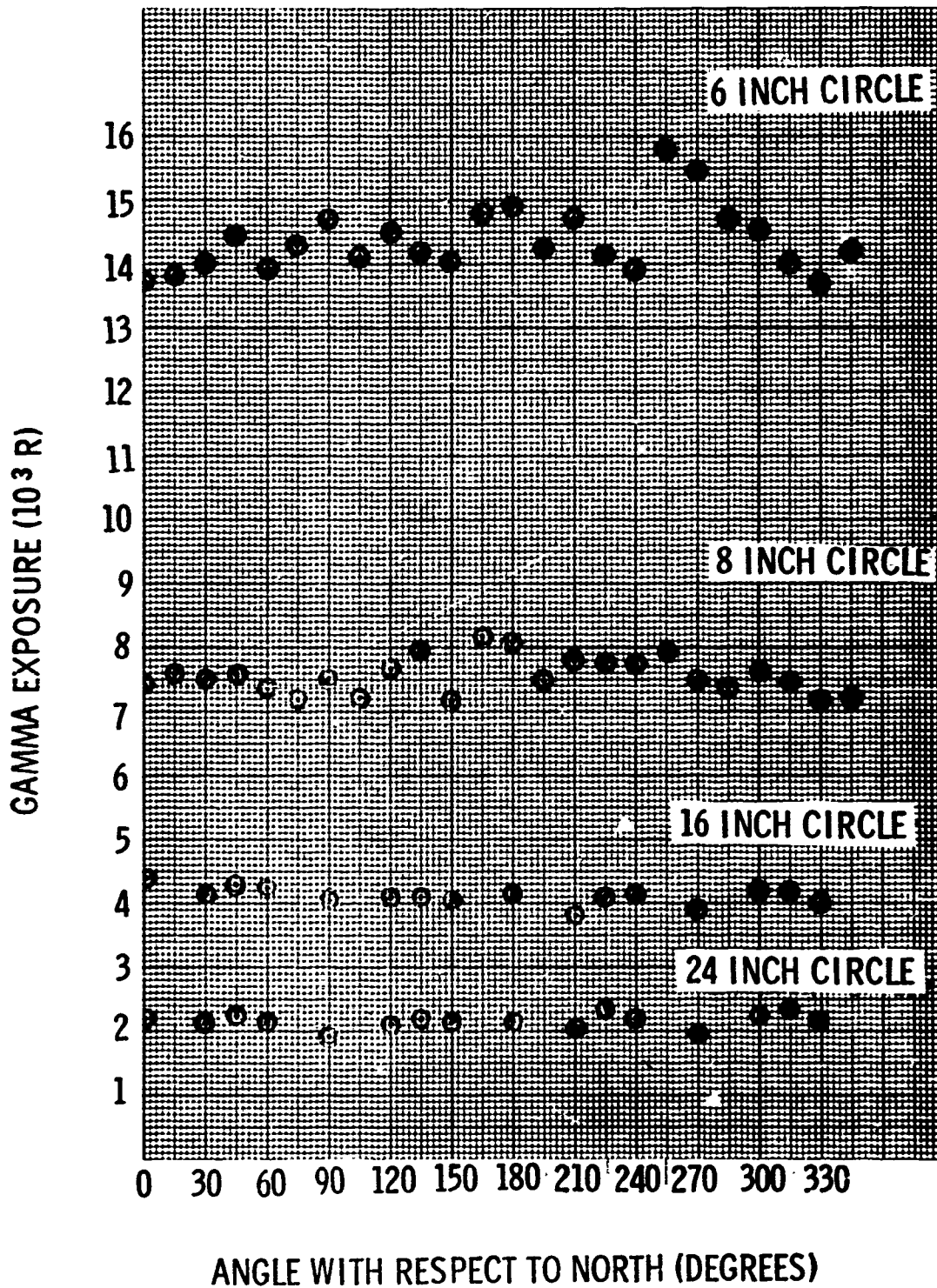
Figure I-14 Gamma dose-rate as a function of radial distance from the core centerline.

Legend:
- o PIN diode, 70 μs FWHM
- $\triangle$ MC - 1546 diode, 40 μs FWHM
- — Calculated, 40 μs FWHM

Y-axis: GAMMA DOSE - RATE (RAD - H_2O / SEC.)

X-axis: RADIAL DISTANCE FROM CORE CENTERLINE (INCHES)

Cadmium Safety Shield
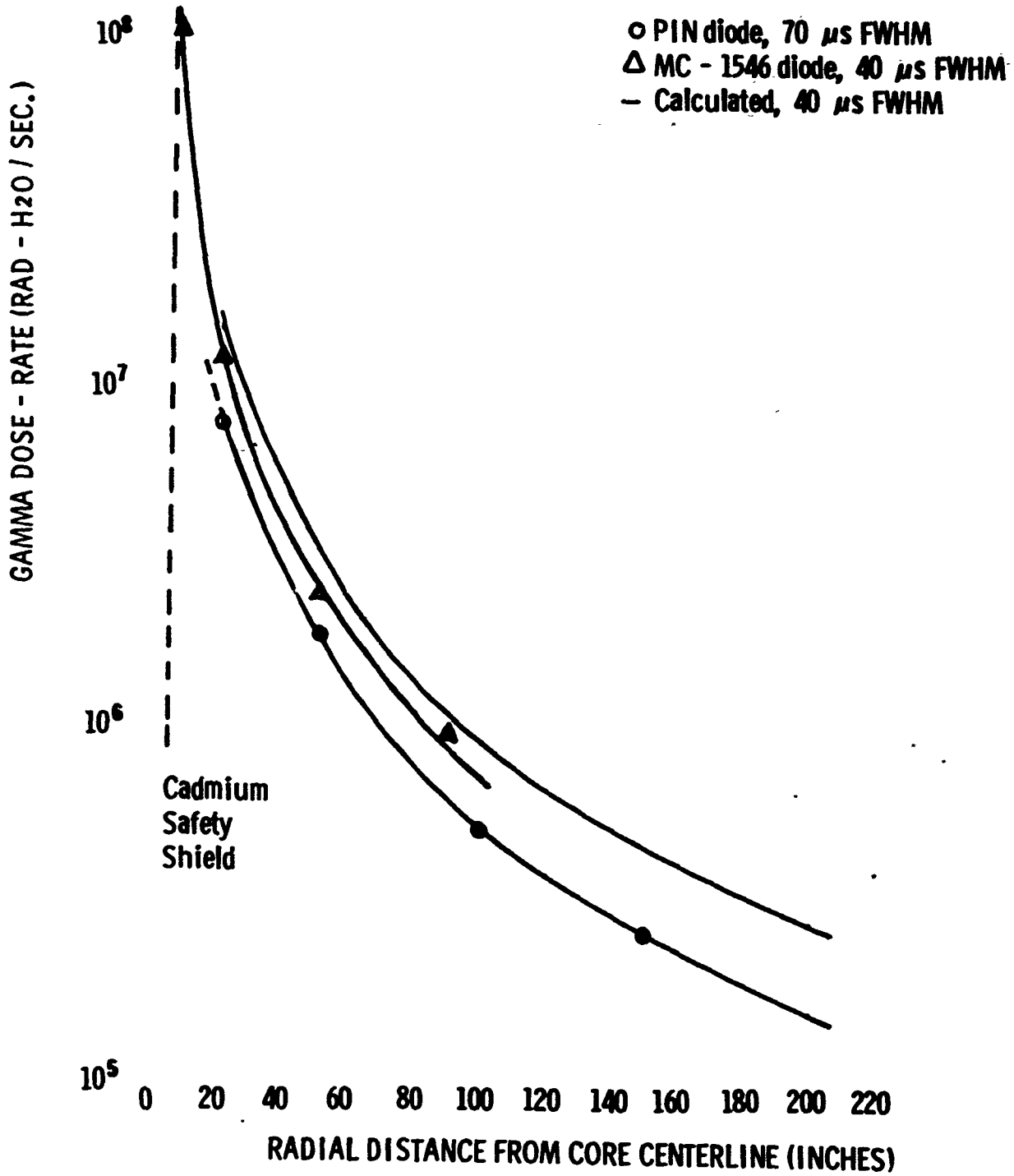
Figure I-15 Peak core temperature vs. time for several power levels.

TIME (MIN.)

TEMPERATURE, TC-] (°C)

MAXIMUM OPERATING TEMPERATURE – 325 °C

10.7 KW
8.5 KW
6.4 KW
5.1 KW
4.4 KW
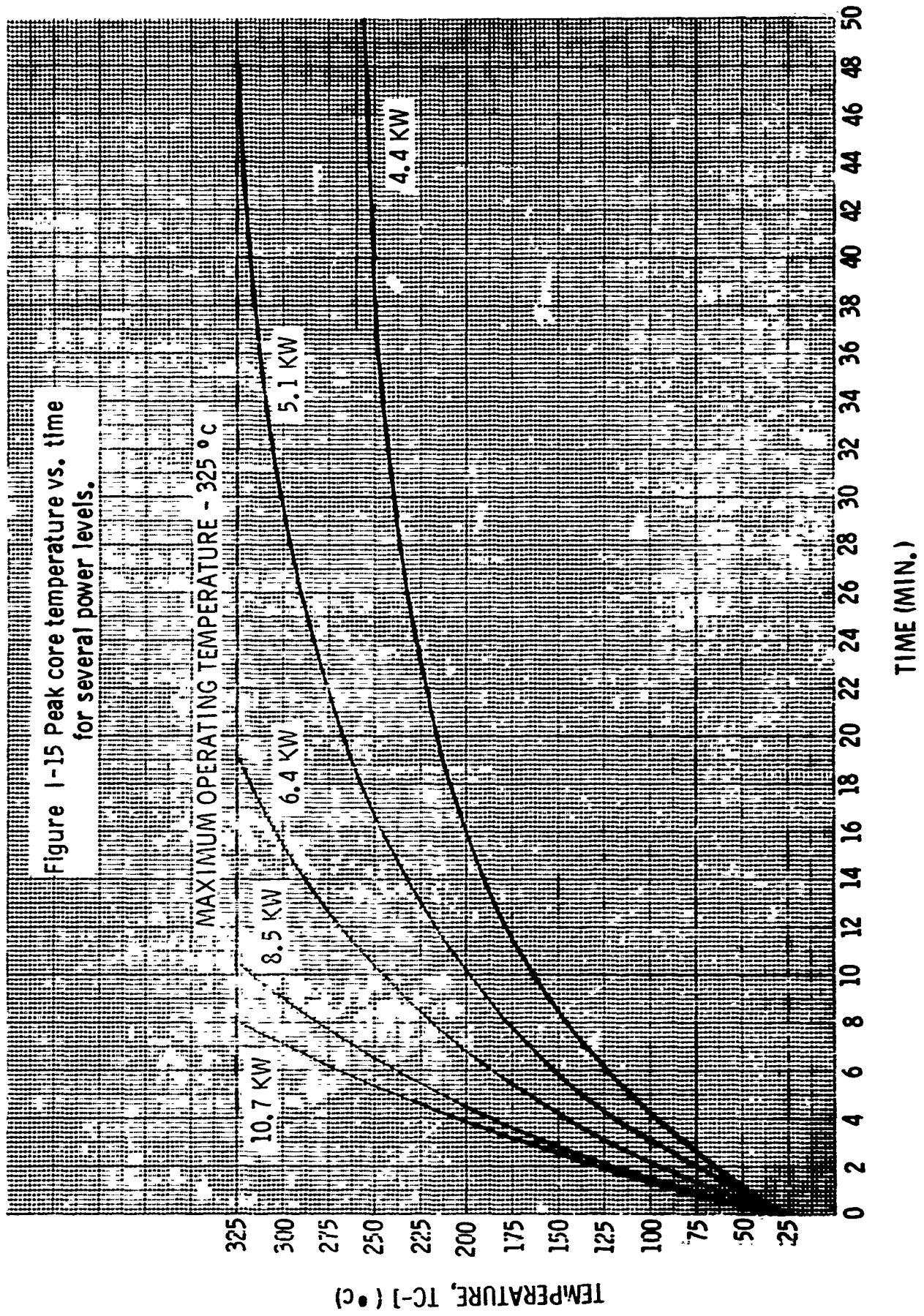
APPENDIX II. REFERENCES

LITERATURE CITED

1. T. Wimett, "DDK Calculation of FBR Core Fission Density, " Los Alamos Scientific Laboratory, 1964

2. K. C. Humpherys, et al, "Nuclear Radiation Dosimetry Measurements of the White Sands Missile Range Fast Burst Reactor, " EG&G. Report 5-26Z-R, Jan 65

3. H. M. Murphy, "Summary of Neutron and Gamma Dosimetry Techniques, " Air Force Weapons Laboratory Technical Report No. AFWL-TR-66-111, Sep 67

4. J. Meason and H. Wright, Work Performed for Nuclear Effects Directorate, WSMR, 1969

5. J. A. Halblieb, et al, "Neutron Spectroscopy by Foil Activation in Radiation Effects Studies, " Sandia Corporation Report SC-DC-67-1572, Jul 67

6. J. R. Stehn, et al, "Neutron Cross Sections, " Brookhaven National Laboratory, BNL-325 Supplement No. 2, 1964

7. A. De La Paz, D. L. Welch, T. F. Luera, and J. D. Parkyn, "Operating Experience and Neutron Fluence Characteristics of the White Sands Missile Range Fast Burst Reactor, " Trans. Amer. Nucl. Soc. , Vol 11, No. 2, pp 645-646, 1968

8. T. Wimett, et al, "Godiva II — An Unmoderated Pulse-Irradiation Reactor, " Nuclear Science and Engineering, Vol 8, pp 691-708, 1960

9. M. Farkas and E. Eldridge, "Heat Contents and Specific Heats of Some Uranium-Bearing Fuels, " Journal of Nuclear Materials, Vol 27, pp 94-96, 1968

10. R. L. Long, Nuclear Engineering Department, University of New Mexico, Private Communication, Sep 69

11. J. Meason and H. Wright, Nuclear Effects Directorate, WSMR, Private Communication, Apr 69

12. R. L. Long, "Effects of Reflectors on the Burst Characteristics of an Enriched Uranium - 10 w/o Molybdenum Alloy Fast Burst Reactor," Internal Memo 26, Missile Science Division, Army Missile Test and Evaluation Directorate WSMR, 1965

13. R. L. Coats, "Neutron Kinetics of a Reflected Fast Burst Reactor," Sandia Laboratories Report SC-RR-67-802, Dec 67

14. R. L. Coats and P. D. O'Brien, "Pulse Characteristics of Sandia Pulsed Reactor-II," Trans. Amer. Nucl. Soc., Vol 11, No. 1, pp 219-220, Jun 68

15. T. Luera, FBR Technical Memo 69-8, WSMR, Mar 69

16. "Technical Specifications for the WSMR Fast Burst Reactor Facility," Nuclear Effects Division, Missile Science Directorate, Army Missile Test and Evaluation, WSMR, Sep 66

SELECTED BIBLIOGRAPHY

1. Memorandum, "Characteristics of Nuclear Effects Branch Radiation Facilities and Operational Procedures," Army Missile Test and Evaluation, WSMR, Mar 66

2. K. C. Humpherys, "A Review of Some Passive Dosimetry Methods Used in Radiation Effects Studies with Fast Burst Reactors," AEC 15 Symposium Series, Fast Burst Reactors, US Atomic Energy Commission Division of Technical Information, Oak Ridge, Tennessee, Dec 69

APPENDIX III. DISTRIBUTION LIST

Addresse	Number of Copies

Commanding General
US Army Test and Evaluation Command
Aberdeen Proving Ground, Maryland 21005
ATTN: AMSTE-PO-M   (NO STAMP)   15
          AMSTE-NB (R. Galasso)   3

Commanding General
US Army Materiel Command
Washington, D. C. 20315
ATTN: AMCRD-SE   3
          AMCS-N   3
          AMCRD-BN   3

Commanding Officer   3
US Army Aviation Material Laboratories
ATTN: OSMFE-CPR
Fort Eustis, Virginia 23604

Commanding General   3
US Army Electronics Command
ATTN: AMSEL-PP-PAD
Fort Monmouth, New Jersey 07703

Commanding General   3
US Army Tank-Au')motive Command
ATTN: SMOTA-R T
Warren, Michigan ±8090

Commanding Officer   3
Aberdeen Proving Ground
ATTN: STEAP-DS-TA
Aberdeen Proving Ground, Maryland 21005

Addressee	Number of Copies
Commanding Officer Deseret Test Center ATTN: STEPD-PA(S) Bldg 100 Soldiers Circle Fort Douglas, Utah 84113	3
President US Army Airborne, Electronics and Special Warfare Board ATTN: STEBF-AP-L Fort Bragg, North Carolina 28307	3
President US Army Air Defense Board ATTN: STEBD-PO Fort Bliss, Texas 79916	3
Commanding Officer US Army Arctic Test Center ATTN: STEAC-TA APO Seattle 98733	3
President US Army Armor and Engineering Board ATTN: STEBB-EX-R Fort Knox, Kentucky 40121	3
President US Army Artillery Board ATTN: STEBA-OP Fort Sill, Oklahoma 73504	3
President US Army Aviation Test Board ATTN: STEBG-AS Fort Rucker, Alabama 36360	3

Addressee	Number of Copies
President US Army Infantry Board ATTN: STEBC-OP Fort Benning, Georgia 31905	3
Commanding Officer US Army General Equipment Test Activity ATTN: STEGE-CP (TA&O) Fort Lee, Virginia 23801	3
Commanding General US Army Electronic Proving Ground ATTN: STEEP-T Fort Huachuca, Arizona 85611	10
Commanding Officer US Army Tropic Test Center APO New York 09827 ATTN: STETC-TE STETC-RE	2 2
Commanding Officer Yuma Proving Ground ATTN: STEYP-TE Yuma, Arizona 85364	10
Commanding Officer US Army Aviation Test Activity ATTN: STEAV-PO Edwards Air Force Base, California 93523	3
Commanding Officer Jefferson Proving Ground ATTN: STEJP-TD Madison, Indiana 47251	3
President US Army Maintenance Board Fort Knox, Kentucky 40121	3

Addressee	Number of Copies
Chief, Nuclear Research Laboratory Army Materials Research Agency Watertown Arsenal Watertown, Massachusetts 02172	3
Diamond Ordnance Radiation Facility Harry Diamond Laboratories ATTN: W. Giesler Washington, D. C. 20425	3
Ballistics Research Laboratories Army Pulse Radiation Facility Aberdeen Proving Ground, Maryland 21005	3
Chief of Engineers Department of the Army ATTN: ENGSO Washington, D. C. 20315	3
Director, US Army Engineers Reactors Group Department of the Army Fort Belvoir, Virginia 22060	3
Commander (include DDC Form 50) Hq, Defense Documentation Center for Scientific and Technical Information ATTN: Document Service Center Cameron Station Alexandria, Virginia 22314	20

Commanding General
White Sands Missile Range, New Mexico 88002
ATTN: AD-R (Copy 1 stamped Record Copy)   1
      TE-P (Copies 2 and 3 for Reference Files)   22
        (Prerelease Copy)   1
      RE-L   3

Total   161

DOCUMENT CONTROL DATA - R & D

(Security classification of title, body of abstract and indexing annotation must be entered when the overall report is classified)

1. ORIGINATING ACTIVITY (Corporate author)	2a. REPORT SECURITY CLASSIFICATION
Army Missile Test and Evaluation White Sands Missile Range, New Mexico	Unclassified
	2b. GROUP

3. REPORT TITLE

METHODOLOGY INVESTIGATION: OUTPUT CHARACTERISTICS OF THE WHITE SANDS MISSILE RANGE FAST BURST REACTOR

4. DESCRIPTIVE NOTES *(Type of report and inclusive dates)*

Final Report, July 1968 to March 1970

5. AUTHOR(S) *(First name, middle initial, last name)*

Ted F. Luera and Don L. Welch

6. REPORT DATE	7a. TOTAL NO. OF PAGES	7b. NO. OF REFS
Apr 70	67	18

8a. CONTRACT OR GRANT NO.	9a. ORIGINATOR'S REPORT NUMBER(S)
b. PROJECT NO. USATECOM Project 9-CO-005-000-002	None
c. RDT Project 1S665702D625-05	9b. OTHER REPORT NO(S) (Any other numbers that may be assigned this report)
d.	None

10. DISTRIBUTION STATEMENT

Each transmittal of this document within US Army Materiel Command must have prior approval of CG, USATECOM, ATTN: AMSTE-TS, Aberdeen Proving Ground, Maryland 21005. Each transmittal of this document outside US Army Materiel

11. SUPPLEMENTARY NOTES Command must have prior approval of CG, US Army Materiel Command, ATTN: AMCPA-S, Washington, DC 20315	12. SPONSORING MILITARY ACTIVITY Commanding General USATECOM, Aberdeen Proving Ground, Maryland, ATTN: AMSTE-PO

13. ABSTRACT

The results of neutron and gamma radiation dosimetry measurements are presented in this report. Sufficient data are provided so that estimates of the neutron fluence, neutron spectrum, gamma dose, and gamma dose rate can be obtained for both burst operations and power runs.

A discussion of the dosimetry techniques presently in use at the Nuclear Effects Directorate is presented, as are means of improving and expanding upon these techniques.

A summary of those factors which affect burst yield or maximum power level is also provided.

DD FORM 1473 REPLACES DD FORM 1473, 1 JAN 64, WHICH IS OBSOLETE FOR ARMY USE.

KEY WORDS	LINK A		LINK B		LINK C	
	ROLE	WT	ROLE	WT	ROLE	WT
Dosimetry						
Reactor						
Fast Burst Reactor						